

NASA Contractor Report 187136

1N-08
36335
P-74

Compensation of Distributed Delays in Integrated Communication and Control Systems

Asok Ray and Rogelio Luck
The Pennsylvania State University
University Park, Pennsylvania

(NACA-CR-117136) COMPENSATION OF
DISTRIBUTED DELAYS IN INTEGRATED
COMMUNICATION AND CONTROL SYSTEMS Final
Report (Pennsylvania State Univ.) 74 p
CSCC 010 65/08 0036335
N91-22193
unclas

August 1991

Prepared for
Lewis Research Center
Under Grant NAG3-823

NASA
National Aeronautics and
Space Administration

COMPENSATION OF DISTRIBUTED DELAYS IN INTEGRATED COMMUNICATION AND CONTROL SYSTEMS

ABSTRACT

Advances in aircraft and spacecraft technology demand high-speed and reliable communications between the individual components and subsystems for decision-making and control. This can be accomplished by Integrated Communication and Control Systems (ICCS) which use asynchronous time-division-multiplexed networks. Unfortunately, these networks can introduce randomly varying distributed delays. This paper presents the concept, analysis, implementation, and verification of a method for compensating delays that are distributed between the sensor(s), controller, and actuator(s) within a control loop. With the objective of mitigating the detrimental effects of these network-induced delays, a predictor-controller algorithm has been formulated and analyzed.

Robustness of the delay compensation algorithm is investigated relative to parametric uncertainties in plant modeling. The delay compensator has been experimentally verified on an IEEE 802.4 network testbed for velocity control of a DC servomotor. Dynamic performance of the delay compensator has also been examined by combined discrete-event and continuous-time simulation of the flight control system of an advanced aircraft, that uses the Society of Automotive Engineers (SAE) linear token passing bus for data communications. The paper is concluded with several areas of future research in the evolving field of ICCS.

TABLE OF CONTENTS

	Page
ABSTRACT	i
LIST OF FIGURES	iv
1. INTRODUCTION	1
1.1. Benefits of the Reported Research	4
1.2. Summary of Previous Research in ICCS	5
1.3. Contributions of the Technical Report	6
1.4. Organization of the Technical Report	7
2. OBSERVER FOR ESTIMATION OF DELAYED STATES	9
3. ALGORITHM OF THE OBSERVER-BASED DELAY COMPENSATOR	12
4. MODELING UNCERTAINTY OF TWO-STEP PREDICTOR/CONTROLLER	18
5. EXPERIMENTAL VERIFICATION AT A NETWORK TESTBED	23
5.1. Experimental Setup #1: Velocity Control with Constant Delays	28
5.2. Experimental Setup #2: Velocity Control with Random Delays	35
6. SIMULATION OF A FLIGHT CONTROL SYSTEM	38
7. SUMMARY, CONCLUSIONS, AND RECOMMENDATIONS FOR FUTURE RESEARCH	45
APPENDIX A: EXTENDED OBSERVABILITY UNDER RECURRENT LOSS OF OUTPUT DATA	52
A.1. Extended Observability: Concepts and Test Criteria	53
APPENDIX B: LEMMAS FOR PROPOSITION 3	61
APPENDIX C: STABILITY OF THE DELAY-COMPENSATED SYSTEM	65
REFERENCES	67

LIST OF FIGURES

Figure 1-1. Schematic Diagram for ICCS Network	2
Figure 3-1. Schematic Diagram of the p-Step Delay Compensation Algorithm	15
Figure 5-1: Schematic Diagram of the Experimental Facility	26
Figure 5-2: Dynamic Response of the Motor: Fixed Delay = 0, Reference Velocity = 16 rad/sec	30
Figure 5-3: Dynamic Response of the Motor: Fixed Delay = T, Reference Velocity = 15 rad/sec	33
Figure 5-4: Dynamic Response of the Motor: Fixed Delay = 2T, Reference Velocity = 13.5 rad/sec	34
Figure 5-5: Dynamic Response of the Motor: Random Delay = 2T, Reference Velocity = 18 rad/sec	37
Figure 6-1: Block Diagram of the Flight Control System . . .	39
Figure 6-2: Dynamic Response of Pitch Rate	43

1. INTRODUCTION

Large-scale dynamical systems, such as advanced aircraft and spacecraft, require reduction of direct human intervention in control and decision-making processes and its replacement by hierarchical levels of automatic control [1] as much as practicable. In this respect, much effort is being focused on integration of expert systems, i.e., rule-based procedures, with model-based algorithms within the control loops. Such a multi-loop, intelligent control system requires extensive interactions between its disparate and spatially distributed subsystems and components. Such interactions, especially when the devices are not collocated, can be effectively carried out via an asynchronous time-division-multiplexed data communication network [2]. This concept of Integrated Communication and Control Systems (*ICCS*) has already been adopted in aeronautics and astronautics [3], computer-integrated manufacturing (*CIM*) [4], and is being actively pursued for integrated control of chemical processes [5] and future generation automobiles [6]. A general concept of how distributed delays are induced by an *ICCS* network is illustrated in Figure 1-1.

The tasks of decision making, e.g., fault detection, isolation and reconfiguration (FDIR), at the system level are simplified within the common network environment of *ICCS*. The reason is that monitoring of status and dynamic behavior of the integrated control system becomes a relatively less difficult task due to availability

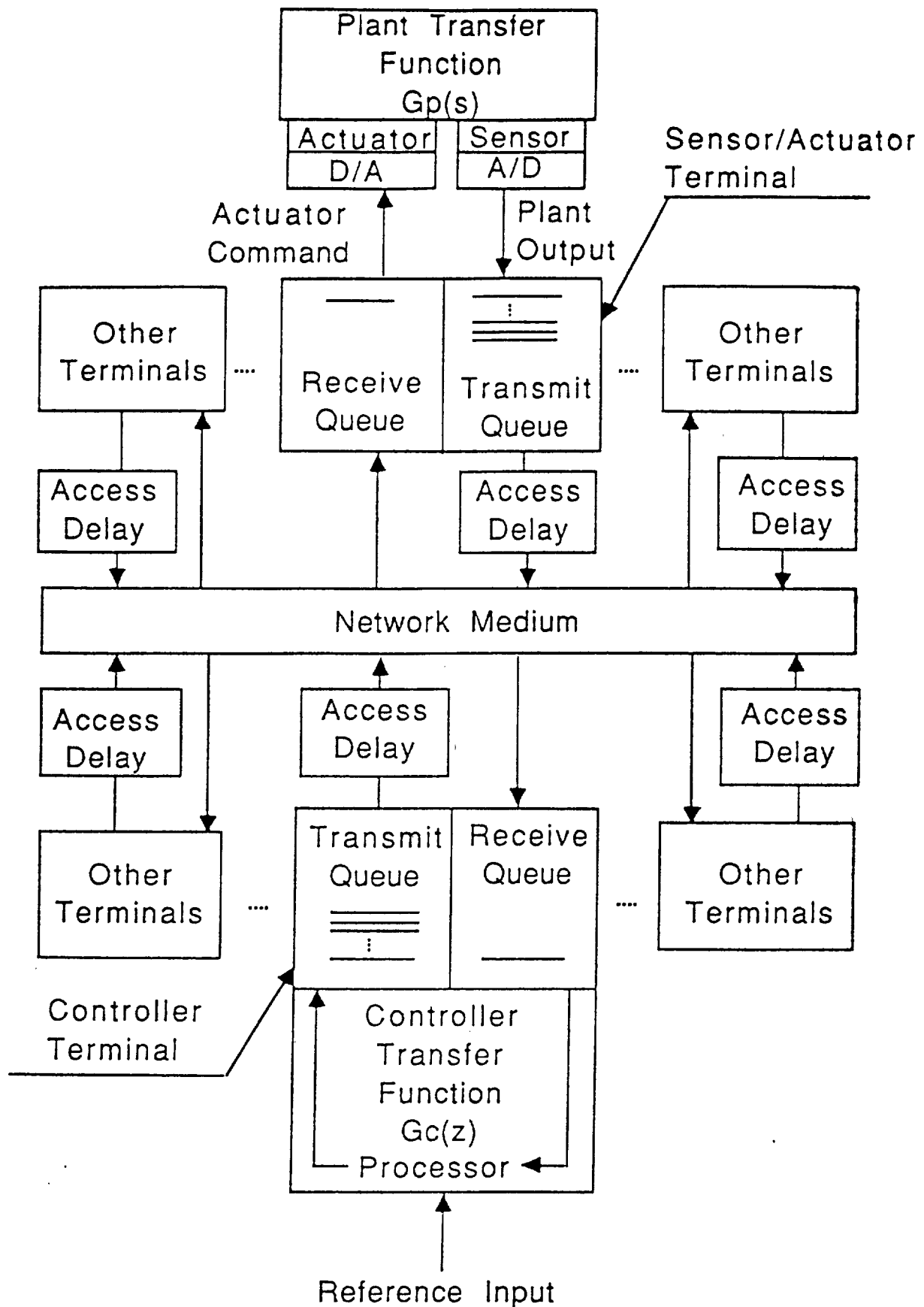


Figure 1-1. Example of an Integrated Communication and Control System

of the information that traverses throughout the communication network. This is of paramount importance in strategic processes like advanced aircraft and spacecraft. For example, a contingency plan may be implemented by reconfiguring the system software to compensate for failures. An additional advantage of using a network in FDIR is the convenient use of analytical redundancy (i.e., analytically deduced measurement(s) of a plant variable) to supplement the sensory information as well as for identifying common mode failures [7,8,9]. The above concept is also applicable to factory automation [10] in computer-integrated manufacturing (CIM) and integrated vehicle control systems in future generation automobiles.

The network traffic in *ICCS* is heterogeneous in the sense that both real-time (e.g., flight critical) and some of the non-real-time (e.g., avionics) functions are likely to share a common data bus. This would generate aperiodic and possibly random traffic in the network. The sensor and control signals in *ICCS* are subjected to randomly varying distributed delays although the average bus load is kept well below the saturation level [11-13]. These delays occur in addition to the sampling time and data processing delays. Furthermore, the *ICCS* could be subjected to recurrent loss of data due to noise corruption in the communication medium and malfunctions of the network protocol. Therefore, an observable (reachable) system that assumes availability of sensor (control) data at consecutive samples may become unobservable (unreachable) due to recurrent loss of data. If the plant is unstable in the open loop as it could be

for highly maneuverable supersonic aircraft, then closed loop stability requires the system to be detectable and stabilizable. This is ensured by complete observability and reachability [14]. Recurrent loss of data could render the system undetectable and/or unstabilizable. Of importance are the conditions for which this phenomenon could lead to loss of observability (reachability) [15,16] and therefore be a source of potential instability. This subject is discussed in depth in Appendix A.

There are two parallel but complementary approaches to circumvent the problem of network-induced delays and loss of data:

Approach #1: Selection of a reliable communication protocol that will prioritize *real-time* traffic (e.g., sensor and control data for fast loops, and interrupt signals for event synchronization) by preempting the *non-real-time* traffic (e.g., aircraft systems operation and management data). An example is the fiber-optic version of the Society of Automotive Engineers (SAE) token bus protocol [17] that allows four levels of priority at a transmission speed of 100 Mbps and a high level of noise immunity. An appropriate protocol and a carefully designed network would certainly reduce the induced delays and the probability of data loss but their detrimental effects cannot be completely eliminated especially if the dynamic performance requirements of the control system are stringent or the bus utilization is not exceedingly low. ■

Approach #2: Compensation of network-induced delays by: (i) modification of the existing control systems (that are designed for conventional digital control systems) by updating their parameters and incorporating additional observers/predictors, or (ii) development of a new control structure. This approach assumes that the distribution of the network traffic and the specifications of the access protocol are given, i.e., the statistical characteristics of the network-induced delays and the probability of data loss are assumed to be known from the point of view of ICCS design. ■

1.1. Benefits of the Reported Research

Although significant efforts have been expended for improving the speed, reliability and other performance of computer networks, and ample research papers have been published in the areas of modeling and simulation of computer communication protocols, significance of network-induced delays and data loss relative to stability of

feedback control systems has not apparently received much consideration. Therefore, the approach #2 has been adopted in the reported research to deal with *ICCS* assuming that the network is well-designed using the approach #1. *ICCS* design via a combination of these two approaches will yield the following advantages:

- o Augmentation of operational flexibility and system reliability without increasing the network and computer hardware redundancy;
- o Enhancement of bus utilization, thereby, allowing incorporation of advanced control algorithms and AI-based decision support systems within the existing network and computer system;
- o Robustness of the integrated control system relative to noise, transient traffic, and malfunctions of the network, and uncertainties and disruptions in plant operation;
- o Reconfiguration of the control structure and self-repair (in the event of several unattended failures) via software migration over the network.

1.2. Summary of Previous Research in *ICCS*

The potential problem of network-induced delays in *ICCS* has been addressed in a sequence of three papers [11-13] under the NASA LeRC Grant No. NAG 3-823. In the first paper [11], a finite-dimensional model of *ICCS* is presented by taking into consideration the effects of network-induced delays. A necessary and sufficient condition for system stability was established for the special case of periodically varying (non-random) delays. Attention was focused on the control loops with identical sampling rates for the sensor and controller with a time skew Δ_s between the respective sampling instants. Although this model is more suitable for analysis of dynamic performance than other infinite-dimensional models [11], its application to stability analysis for non-periodically and randomly varying delays is not straight-forward. The second paper [12] discusses the issues related to *ICCS* design with an emphasis on how

Δ_s can significantly contribute to network-induced delays and distort the control command sequence due to *vacant sampling*. An alternative approach, by which *vacant sampling* can be avoided, is to deliberately assign non-identical sampling periods T_s and T_c to the sensor and controller, respectively. The third paper [13] specifically addresses finite-dimensional modeling of control systems that have non-identical sensor and controller sampling rates and are subjected to randomly varying distributed delays. Criteria for selection of the sampling ratio T_s/T_c were presented for this special class of multi-rate sampling.

1.3. Contributions of the Technical Report

This report presents the concept, algorithm, and experimental and simulation results of a delay compensation algorithm for *ICCS* with identical sensor and controller sampling rates. The proposed delay compensator is intended to alleviate the detrimental effects of network-induced delays by using a multi-step predictor. The key idea in the compensator design is to monitor the data when it is generated and to keep track of the delay associated with it. With this knowledge, an algorithm keeps the delay constant as seen by the controller. Therefore, the closed loop control system model is constrained to be finite-dimensional, linear, time-invariant provided that the plant, observer, and controller are linear time-invariant. Therefore, this delay-compensated system model is more suitable for stability analysis of *ICCS* than the time-varying model reported in our previous publication [11].

The major assumption in the above delay compensation algorithm is that the (randomly varying) network-induced delays are bounded. This assumption is justified in view of the fact that unbounded delays would render the feedback loop open. Using a specified confidence interval, an upper bound can be assigned to each of these randomly varying delays. The number of predicted steps in the compensator is then determined from these bounds, and the compensated system may use the original control law that was designed for the system without being subjected to the induced delays. The contributions of this report are:

- o Formulation of the concept of a delay compensation strategy for *ICCS*;
- o Establishment of the separation principle for the multi-step predictor and state-variable feedback controller;
- o Analysis of some of the robustness properties of the delay compensator relative to plant modeling uncertainties; and
- o Implementation of the delay compensation strategy, and its testing by:
 - Experimentation with a servomotor control system at a network testbed that employs the IEEE 802.4 token bus as the medium access control protocol;
 - Simulation of the flight control system of an advanced aircraft using an SAE token bus network.

1.4. Organization of the Technical Report

The report is organized in seven sections and three appendices. The concept of using an observer for delay compensation and contributions of other researchers in this field are succinctly presented in Section 2. The delay compensation algorithm is derived in a closed loop representation in Section 3. Robustness analysis relative to modeling uncertainties is presented in Section 4 for a two-step delay compensator. A description of the experimental

facility, details of the experiments, and interpretation of the experimental results are presented in Section 5. A functional description of the simulation program and a model of the simulated flight control system are presented in Section 6 along with a discussion and interpretation of the simulation results. The report is concluded in Section 7 with recommendations for future research to deal with the basic problems of stability analysis and robust design of the delay-compensated system.

Appendix A presents the concept of extended observability in the event of recurrently random data loss, followed by pertinent results. Appendix B provides the supporting materials for proof of the delay compensation algorithm in Section 3. Stability of the delay-compensated system in presence of plant modeling uncertainties is discussed in Appendix C.

2. OBSERVER FOR ESTIMATION OF DELAYED STATES

The sensor, controller, and actuator are assumed to have identical sampling rates. Furthermore, we assume the sensor and actuator to be synchronized, i.e., the time skew between their sampling instants is maintained at zero. Under these conditions, the plant and controller dynamics of the delayed system at the sample time k are modeled as:

$$x_{k+1} = A x_k + B u_{k-\Upsilon(k)} \quad \text{-plant dynamics with delayed control (2-1)}$$

$$y_k = C x_k \quad \text{-sensor measurement (2-2)}$$

$$w_k = y_{k-\Delta(k)} \quad \text{-delayed output (2-3)}$$

$$u_k = \xi(w_k) \quad \text{-control function (2-4)}$$

where $x \in \mathbb{R}^n$, $u \in \mathbb{R}^s$ and $y \in \mathbb{R}^m$, and the matrices A , B , and C are of compatible dimensions; the finite non-negative integers $\Upsilon(k)$ and $\Delta(k)$ represent the numbers of delayed samples in control inputs and measurements, respectively. The control law u_k is a linear function of the history $W_k := \{w_k, w_{k-1}, \dots\}$ of the delayed measurements. The plant in (2-1) and (2-2) is reachable and observable. The objective is to construct the control function ξ such that the effects of the delays on the control system are mitigated.

Remark 2.1: It has been stated in Section 1 that the (randomly varying) network-induced delays are assumed to be bounded. Therefore, for the purpose of delay compensator design, Υ and Δ may be treated as upper bounds (in units of sampling periods) for the controller-actuator and sensor-controller delays, respectively. In contrast, the delays in the *ICCS* model reported in our previous work [11,12] are deterministically or randomly varying. ■

Several investigators have addressed the problems of delay compensation in closed loop control systems. An intuitive approach [18] is to augment the system model to include delayed variables as additional states. Unfortunately, this renders some of the states uncontrollable even when the original system is completely controllable [19,20]. For the case of delayed control inputs, Pyndick [21] proposed a predictor for the optimal state trajectory based on past control inputs. Zahr and Slivinsky [22] considered the problem of controlling a computer-controlled system with measurement and computational delays. It was pointed out that the delays in multivariable systems may result in: (i) an increase in the magnitudes of the transients, and poor response during the inter-sampling time; (ii) loss of decoupling between individual SISO control loops although decoupling may be restored for a stable process at the steady state; and (iii) a possible decrease in stability margin. Their algorithm was verified by simulation but the use of an observer to estimate the unavailable states was not discussed.

A significant amount of research work has been reported for observer and controller design [20,23,24] for the case of inherent constant delays that occur within the process to be controlled. In contrast to the system, under consideration in (2-1) to (2-4) where the sensor and control data are delayed, such processes are described as follows:

$$\dot{x}(t)/dt = A x(t) + D x(t-h) + G u(t) \quad (2-5)$$

$$y(t) = C x(t) \quad (2-6)$$

where h is a constant. By setting $G=0$ and $D=BF$ in (2-5) (where F is the gain matrix), it reduces to a delayed state-variable-feedback system.

The reported literature in delay compensation does not apparently address the problem of distributed delays in both the input and output variables, which is the case with ICCS. A possible approach [22] for compensation of constant delays that affect the input or output variables of a system is to predict the current output. However, if a state-space approach is used for predicting the output, the plant state variables must be obtained first. Moreover, the measurements might be corrupted with noise. In view of the above, we propose to use an observer for estimation of the delayed states and then to predict the current state using the state transition matrix. However, this multi-step observer would impose additional dynamics which generate additional phase lag in the control system. The impact of this phase lag on the system dynamic performance should not be significant because the controller is expected to be designed with a sufficiently large stability margin to allow for disturbances and uncertainties.

The observer parameters can be optimally selected to attenuate the high-frequency noise in the measurements. If the measurement noise is considerable, then the proposed algorithm could be extended to include a stochastic filter [25] instead of a deterministic observer. Furthermore, a reduced order observer or a functional observer [26] can be used to reduce the observation lag.

3. ALGORITHM OF THE OBSERVER-BASED DELAY COMPENSATOR

The algorithm for compensation of distributed delays is built upon the concept of linear state-variable feedback control and multi-step prediction where no loss of sensor or control data is taken into account. The algorithm is presented below as a proposition.

Proposition 3.1: Given the following predictor-controller scheme:

$$x_{k+1} = Ax_k + Bu_k; \quad y_k = Cx_k \quad \text{Plant Model;} \quad (3-1)$$

$$z_{k+1|1} = Az_{k|1} + Bu_k + L_k(y_k - Cz_{k|1}) \quad \text{Observer Model;} \quad (3-2)$$

$$z_{k+1|r} = Az_{k|r-1} + Bu_k \quad r\text{-Step Predictor for } r \geq 2; \quad (3-3)$$

$$u_k = \Gamma_k z_{k|p} \quad \text{Predictive Control for a fixed } p \geq 2; \quad (3-4)$$

$$\text{where } z_{k|r} := \text{estimate of } x_k \text{ given } (y_{k-r}, y_{k-r-1}, \dots); \quad (3-5)$$

$$e_k := x_k - z_{k|1} \text{ is the estimation error;} \quad (3-6)$$

the gain matrices $\{L_k\}$ and $\{\Gamma_k\}$ are *a priori* determined, and

the initial conditions $z_{0|1}$ and $\{u_i, i=0, \dots, p-1\}$ are given.

Then, the closed loop system equation can be expressed as

$$\begin{pmatrix} x_{k+1} \\ e_{k-p+1} \end{pmatrix} = \begin{pmatrix} (A+B\Gamma_k) & -B\Gamma_k z_k \\ 0 & (A-L_{k-p}C) \end{pmatrix} \begin{pmatrix} x_k \\ e_{k-p} \end{pmatrix}$$

where the plant model is assumed to be exact and

$$3_k := \begin{cases} \prod_{j=1}^p (A - L_{k-p+j-1} C) + \sum_{i=1}^{p-1} [A^{i-1} L_{k-i} C \prod_{j=1}^{p-i-1} (A - L_{k-p+j-1} C)] & \text{if } p \geq 2 \\ I & \text{if } 0 \leq p < 2 \end{cases}$$

Proof: The proof of this proposition is supported by lemma B.1 in Appendix B. Subtracting (3-2) from (3-1) yields

$$\begin{aligned} x_{k+1} - z_{k+1}|_1 &= A(x_k - z_k|_1) - L_k C(x_k - z_k|_1) \\ \text{or } e_{k+1} &= (A - L_k C) e_k \end{aligned} \quad (3-7)$$

Substituting (3-4) in (3-1) and using (B-1.1) from lemma B.1 yields

$$x_{k+1} = Ax_k + B\Gamma_k[z_k|_1 - \sum_{i=0}^{p-2} A^i L_{k-i-1} C e_{k-i-1}] \quad (3-8)$$

Adding and subtracting $B\Gamma_k x_k$ and using (3-6) in (3-8)

$$x_{k+1} = (A + B\Gamma_k)x_k + B\Gamma_k[e_k - \sum_{i=0}^{p-2} A^i L_{k-i-1} C e_{k-i-1}] \quad (3-9)$$

Using (3-7) e_{k+q} for some integer $q \geq 1$ can be expressed as

$$e_{k+q} = [\prod_{j=1}^q (A - L_{k+j-1} C)] e_k \quad (3-10)$$

Replacing e_k and e_{k-i-1} in terms of e_{k-p} , i.e., the use of (3-10) in (3-9) yields

$$x_{k+1} = (A + B\Gamma_k)x_k - B\Gamma_k 3_k e_{k-p} \quad (3-11)$$

$$\text{where } 3_k = \prod_{j=1}^p (A - L_{k-p+j-1} C) + \sum_{i=0}^{p-2} [A^i L_{k-i-1} C \prod_{j=1}^{p-i-1} (A - L_{k-p+j-1} C)]$$

The proof for $p \geq 2$ follows by combining (3-7) and (3-11). If $p=0$ then $3_k = I$ since the delay is zero and the ordinary separation principle is applicable. For $p=1$ the ordinary separation principle still applies since only a first order prediction is used, i.e. $u_k = \Gamma_k z_{k|1}$. In other words, an ordinary linear state feedback controller with observer drives the plant using a first order prediction of the states; thus, a standard observer is naturally suited for compensation of a constant delay of one time step. Thus, if $p=1$ then $3_k = I$. ■

Remark 3.1: If $L_k = L$ and $\Gamma_k = \Gamma$, i.e., constant observer and controller gains, then Proposition 3.1 determines stability of the compensated system due to separation of the controller and the observer. That is, the eigenvalues of the closed loop delayed system are the same as the combined eigenvalues of the two matrices $(A-LC)$ and $(A+B\Gamma)$. ■

The delay compensator is implemented on the basis of *a priori* known upper bounds of the distributed delays that are induced by the ICCS network. These bounds are expressed as integer multiples of the controller sampling period T (which is also the sensor sampling period). The existence of these upper bounds is justified from the point of view of control system design because the control system will be open-loop otherwise. Figure 3-1 shows implementation of the delay compensation scheme in Proposition 3.1. The resulting control system is modeled as follows.

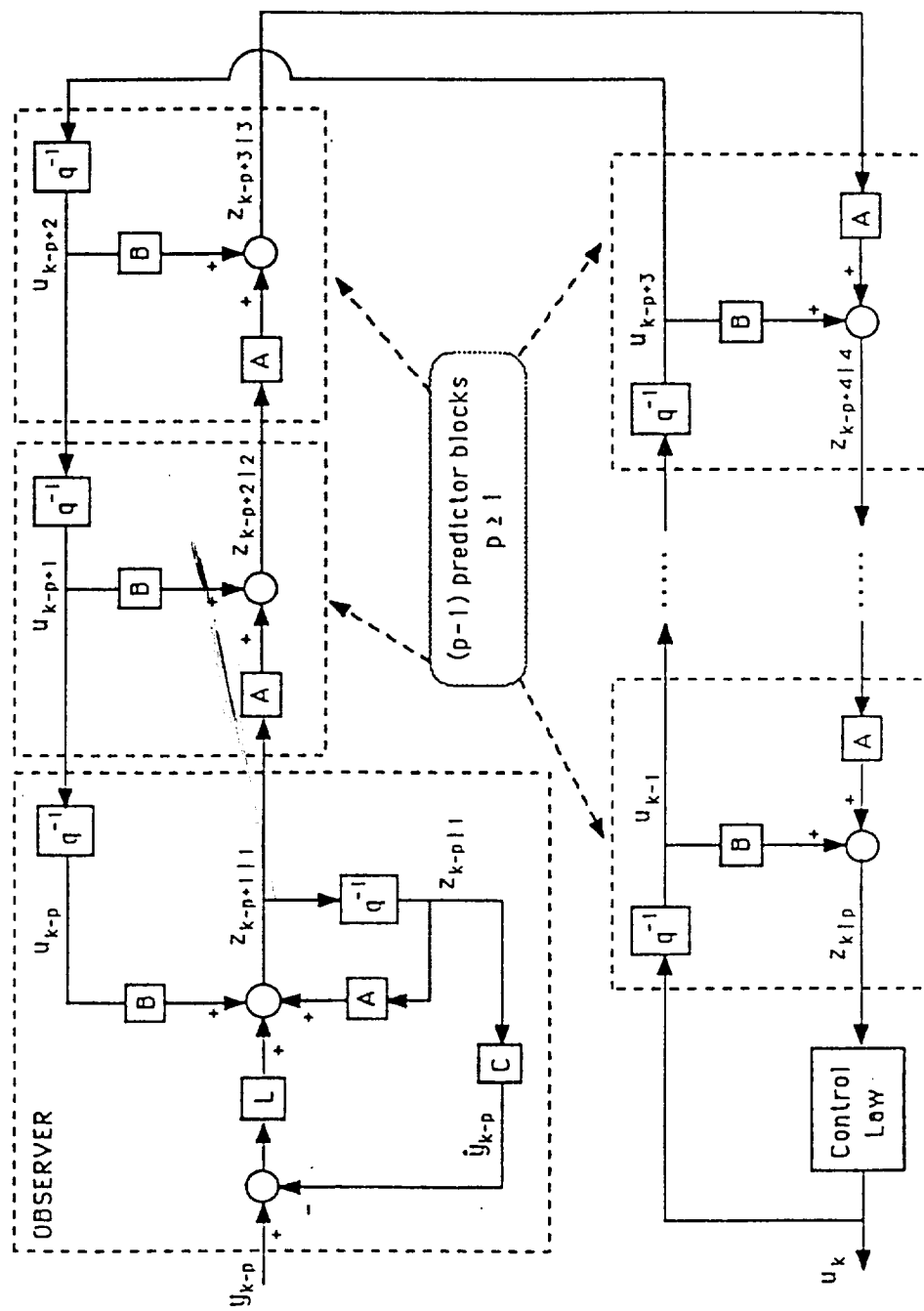


Figure 3-1. Schematic Diagram of the p-Step Delay Compensation Algorithm.

$$w_k = y_{k-p} \quad \text{-delayed sensor data} \quad (1-3)$$

$$z_{k-p+1|1} = (A-LC)z_{k-p|1} + Bu_k + Lw_k \quad \text{-observer dynamics} \quad (1-4)$$

$$z_{k+1|r} = Az_{k|r-1} + Bu_k \quad \text{for } p \geq r \geq 2 \quad \text{-p-step predictor} \quad (1-5)$$

$$u_k = \Gamma z_{k|p} \quad \text{-control law} \quad (1-6)$$

where $x \in \mathbb{R}^n$, $u \in \mathbb{R}^s$ and $y \in \mathbb{R}^m$, the matrices A , B , C , L , and Γ are as defined earlier. The number of predicted steps, p , in the compensator is determined, in general, as the sum of the upper bounds (relative to a specified confidence interval) of the controller-actuator and sensor-controller delays.

Remark 3.2: Loss of sensor and control data is not accounted for in the derivation of the delay compensation algorithm in Proposition 3.1. However, if the network recurrently loses data as it is pointed out in Section 1, the plant may be rendered unobservable or unreachable. Under these circumstances, the notion of observability (reachability) can be extended as explained in detail in [15,16] and Appendix A. If the plant satisfies the condition of extended observability (reachability), then the delay compensator may still function in a possibly degraded mode. Performance analysis of the delay compensator under recurrent loss of data is a subject of future research. ■

Remark 3.3: The number, p , of predicted steps could be obtained as the sum of the specified bounds of the distributed delays, e.g., $\Delta(k)$ and $T(k)$. If the joint statistics of Δ and T are known, p could be calculated more precisely. ■

Remark 3.4: Although the sensor and actuator are assumed to be synchronized, the controller is not required to be synchronized with the sensor or actuator. The time skew between the controller and sensor/actuator sampling instants is absorbed within Δ and T . ■

Remark 3.5: If the sensor and actuator are not collocated, then they can be synchronized by transmitting high priority interrupt signals via the network medium or by additional wiring [12]. Nevertheless this will increase the system reliability requirements. ■

4. MODELING UNCERTAINTY OF A TWO-STEP PREDICTOR/CONTROLLER

In this section we investigate the effects of modeling uncertainty upon performance of the predictor-controller algorithm for the case when the total delay to be compensated is equal to two sampling periods. Let the plant model described in (3-1) have the true dynamical characteristics given as:

$$x_{k+1} = A_k x_k + B_k u_k ; \quad y_k = C_k x_k \quad (4-1)$$

In view of the above the modeling uncertainties are defined as:

$$\delta A_k := A_k - A; \quad \delta B_k := B_k - B; \quad \delta C_k := C_k - C \quad (4-2)$$

Remark 4.1: The postulated model of the plant is time-invariant whereas the uncertainties may be time-varying. ■

The controller structure, given by (3-1)-(3-6) with $p=2$ in (3-4) and steady-state controller gain Γ and observer gain and L , are:

$$u_k = \Gamma z_{k|2} \quad (4-3)$$

$$z_{k+1|1} = A z_{k|1} + B u_k + L(y_k - C z_{k|1}) \quad (4-4)$$

$$z_{k+1|2} = A z_{k|1} + B u_k \quad (4-5)$$

$$e_k = x_k - z_{k|1} \quad (4-6)$$

We intend to obtain a closed loop, augmented state variable representation in such a way that the modeled system dynamics and the modeling errors are decoupled to the maximum possible extent. From now onwards, for the sake of brevity, the subscript k from the time-varying matrices in (4-2) are omitted.

Substituting (4-1) and (4-4) into (4-6) yields

$$\begin{aligned} e_k &= A''x_{k-1} + B''u_{k-1} - [Az_{k-1|1} + Bu_{k-1} + L(C''x_{k-1} - Cz_{k-1|1})] \\ &= \Psi''x_{k-1} - \Psi z_{k-1|1} + \delta Bu_{k-1} \end{aligned} \quad (4-7)$$

where $\Psi'' := A'' - LC''$; $\Psi := A - LC$

Adding and subtracting Ψx_{k-1} in the right hand side of (4-7)

$$e_k = \Psi e_{k-1} + \Theta x_{k-1} + \delta Bu_{k-1} \quad (4-8)$$

where $\Theta := \Psi'' - \Psi = \delta A - L\delta C$

Substituting (4-3) in (4-8) yields

$$e_k = \Psi e_{k-1} + \Theta x_{k-1} + \delta B\Gamma z_{k-1|2} \quad (4-9)$$

Substituting (4-5) in (4-4) yields

$$\begin{aligned} z_{k+1|1} &= z_{k+1|2} + LC''x_k - LCz_{k|1} \\ \text{or } z_{k|2} &= z_{k|1} - LC''x_{k-1} + LCz_{k-1|1} \\ &= x_k - (x_k - z_{k|1}) - LC(x_{k-1} - z_{k-1|1}) - L(C'' - C)x_{k-1} \end{aligned}$$

Substituting (3-6) and (4-2) in the above equation yields

$$z_{k|2} = x_k - e_k - LCe_{k-1} - L\delta Cx_{k-1} \quad (4-10)$$

Substituting (4-9) in (4-10) yields

$$\begin{aligned} z_{k|2} &= x_k - [\Psi e_{k-1} + \Theta x_{k-1} + \delta B\Gamma z_{k-1|2}] - LCe_{k-1} - L\delta Cx_{k-1} \\ &= x_k - (\Psi + LC)e_{k-1} - (\Theta + L\delta C)x_{k-1} - \delta B\Gamma z_{k-1|2} \\ &= x_k - Ae_{k-1} - \delta Ax_{k-1} - \delta B\Gamma z_{k-1|2} \end{aligned}$$

Substituting for $z_{k-1|2}$ in the above equation by using (4-10)

$$\begin{aligned} z_{k|2} &= x_k - Ae_{k-1} - \delta Ax_{k-1} - \delta B\Gamma[x_{k-1} - e_{k-1} - LCe_{k-2} - L\delta Cx_{k-2}] \\ &= x_k - (A - \delta B\Gamma)e_{k-1} - \delta Gx_{k-1} + \delta B\Gamma L\delta Cx_{k-2} + \delta B\Gamma LCe_{k-2} \end{aligned} \quad (4-11)$$

where $\delta G := (\delta A + \delta B\Gamma)$

Substituting for $z_{k-1|2}$ in (4-9) by using (4-11) yields

$$\begin{aligned} e_k &= \Psi e_{k-1} + \Theta x_{k-1} + \delta B\Gamma[x_{k-1} - (A - \delta B\Gamma)e_{k-2} - \delta Gx_{k-2} + \delta B\Gamma L\delta Cx_{k-3} + \delta B\Gamma LCe_{k-3}] \\ &= \Psi e_{k-1} + \delta B_2 e_{k-2} + \delta B_3 e_{k-3} + F_{A \wedge B \wedge C} x_{k-1} + \delta B_1 x_{k-2} + \delta B_C x_{k-3} \end{aligned} \quad (4-12)$$

where $F_{A^{\wedge}B^{\wedge}C} := (\Theta + \delta B\Gamma) = (\delta A - L\delta C + \delta B\Gamma)$

$$\partial_{B1} := -\delta B\Gamma\delta G = -\delta B\Gamma(\delta A + \delta B\Gamma)$$

$$\partial_{BC} := (\delta B\Gamma)^2 L\delta C$$

$$\partial_{B2} := -\delta B\Gamma(A - \delta B\Gamma)$$

$$\partial_{B3} := (\delta B\Gamma)^2 LC$$

Substituting (4-12) into (4-11) yields

$$z_{k|2} = x_k - (A - \delta B\Gamma)[\Psi e_{k-2} + \partial_{B2} e_{k-3} + \partial_{B3} e_{k-4} + F_{A^{\wedge}B^{\wedge}C} x_{k-2} + \partial_{B1} x_{k-3} + \partial_{BC} x_{k-4}] - \delta G x_{k-1} + \delta B\Gamma L\delta C x_{k-2} + \delta B\Gamma L C e_{k-2}$$

Grouping similar terms

$$z_{k|2} = x_k - \delta G x_{k-1} + \partial_{A^{\wedge}B^{\wedge}C} x_{k-2} + \partial_{B4} x_{k-3} + \partial_{B5} x_{k-4} + (\partial_{B6} - A\Psi) e_{k-2} + \partial_{B7} e_{k-3} + \partial_{B8} e_{k-4} \quad (4-13)$$

where

$$\partial_{A^{\wedge}B^{\wedge}C} := -(A - \delta B\Gamma) F_{A^{\wedge}B^{\wedge}C} + \delta B\Gamma L\delta C = -(A - \delta B\Gamma)(\delta A - L\delta C + \delta B\Gamma) + (\delta B\Gamma) L\delta C$$

$$\partial_{B4} := -(A - \delta B\Gamma) \partial_{B1} = (A - \delta B\Gamma) \delta B\Gamma(\delta A + \delta B\Gamma)$$

$$\partial_{B5} := -(A - \delta B\Gamma) \partial_{BC} = -(A - \delta B\Gamma) (\delta B\Gamma)^2 L\delta C$$

$$\partial_{B6} := \delta B\Gamma\Psi + \delta B\Gamma LC = \delta B\Gamma(\Psi + LC) = \delta B\Gamma A$$

$$\partial_{B7} := -(A - \delta B\Gamma) \partial_{B2} = (A - \delta B\Gamma) \delta B\Gamma(A - \delta B\Gamma)$$

$$\partial_{B8} := -(A - \delta B\Gamma) \partial_{B3} = -(A - \delta B\Gamma) (\delta B\Gamma)^2 LC$$

Substituting (4-13) and (4-3) in (4-1) yields

$$x_{k+1} = A'' x_k + B'' \Gamma [x_k - \delta G x_{k-1} + \partial_{A^{\wedge}B^{\wedge}C} x_{k-2} + \partial_{B4} x_{k-3} + \partial_{B5} x_{k-4} + (\partial_{B6} - A\Psi) e_{k-2} + \partial_{B7} e_{k-3} + \partial_{B8} e_{k-4}]$$

Rearranging and grouping similar terms

$$x_{k+1} = Y x_k + D_{A^{\wedge}B} x_{k-1} + D_{A^{\wedge}B^{\wedge}C} x_{k-2} + D_{B1} x_{k-3} + D_{B2} x_{k-4} + Q e_{k-2} + D_{B3} e_{k-3} + D_{B4} e_{k-4} \quad (4-14)$$

where $Y := (A'' + B''\Gamma) = (A + B\Gamma) + \delta G$

$$Q := B''\Gamma(\partial_{B6} - A\Psi) = B''\Gamma(\delta B\Gamma A - A(A - LC))$$

$$D_{A^{\wedge}B} := -B''\Gamma\delta G = -B''\Gamma(\delta A + \delta B\Gamma)$$

$$D_{A^{\wedge}B^{\wedge}C} := B''\Gamma\partial_{A^{\wedge}B^{\wedge}C} = B''\Gamma[(\delta B\Gamma) L\delta C - (A - \delta B\Gamma)(\delta A - L\delta C + \delta B\Gamma)]$$

$$\begin{aligned}
D_{B1} &:= B''\Gamma\partial_{B4} &= B''\Gamma(A-\delta B\Gamma)\delta B\Gamma(\delta A+\delta B\Gamma) \\
D_{B2} &:= B''\Gamma\partial_{B5} &= -B''\Gamma(A-\delta B\Gamma)(\delta B\Gamma)^2 L\delta C \\
D_{B3} &:= B''\Gamma\partial_{B7} &= B''\Gamma(A-\delta B\Gamma)\delta B\Gamma(A-\delta B\Gamma) \\
D_{B4} &:= B''\Gamma\partial_{B8} &= -B''\Gamma(A-\delta B\Gamma)(\delta B\Gamma)^2 LC
\end{aligned}$$

The closed loop equation of the 2-step delayed system follows from (4-12) and (4-14)

$$\begin{bmatrix} x_{k+1} \\ x_k \\ x_{k-1} \\ x_{k-2} \\ x_{k-3} \\ e_{k-1} \\ e_{k-2} \\ e_{k-3} \end{bmatrix} = \begin{bmatrix} Y & D_{A^{\wedge}B} & D_{A^{\wedge}B^{\wedge}C} & D_{B1} & D_{B2} & Q & D_{B3} & D_{B4} \\ I & 0 & 0 & 0 & 0 & 0 & 0 & 0 \\ 0 & I & 0 & 0 & 0 & 0 & 0 & 0 \\ 0 & 0 & I & 0 & 0 & 0 & 0 & 0 \\ 0 & 0 & 0 & I & 0 & 0 & 0 & 0 \\ 0 & 0 & F_{A^{\wedge}B^{\wedge}C} & \partial_{B1} & \partial_{BC} & \Psi & \partial_{B2} & \partial_{B3} \\ 0 & 0 & 0 & 0 & 0 & I & 0 & 0 \\ 0 & 0 & 0 & 0 & 0 & 0 & I & 0 \end{bmatrix} \begin{bmatrix} x_k \\ x_{k-1} \\ x_{k-2} \\ x_{k-3} \\ x_{k-4} \\ e_{k-2} \\ e_{k-3} \\ e_{k-4} \end{bmatrix} \quad (4-15)$$

where the subscripts of elements are chosen to describe their relative dependence on the respective errors in formulating the plant model matrices. The above equation can be separated into the nominal and uncertain parts:

$$X_{k+1} = (V + \delta V) X_k \quad (4-16)$$

where $X_k := [x_k^T \ x_{k-1}^T \ x_{k-2}^T \ x_{k-3}^T \ x_{k-4}^T \ e_{k-2}^T \ e_{k-3}^T \ e_{k-4}^T]^T$,

V is the nominal part which is constant as it contains the constant matrices A , B and C of the plant model in (3-1), and

δV is the uncertainty part which is possibly time-varying because of modeling error matrices δA , δB and δC .

Stability of the above system is discussed in Appendix C.

Remark 4.2: The modeling errors δA , δB and δC constitute a four-fold increase over the order of the augmented system matrix in (4-15). However, by setting $\delta B=0$, the following simplifications result.

$$\partial_{B1}=\partial_{B2}=\partial_{B3}=\partial_{BC}=D_{B1}=D_{B2}=D_{B3}=D_{B4}=0 \text{ and } Y=(A+\delta A+B\Gamma), \quad D_{A \wedge B}=-B\Gamma\delta A, \\ D_{A \wedge B \wedge C}=-B\Gamma A(\delta A-L\delta C), \quad Q=-B\Gamma A(A-LC), \quad F_{A \wedge B \wedge C}=(\delta A-L\delta C).$$

Accordingly the system is reduced with $\delta B=0$ as follows

$$\begin{bmatrix} x_{k+1} \\ x_k \\ x_{k-1} \\ e_{k-1} \end{bmatrix} = \begin{bmatrix} A+\delta A+B\Gamma & -B\Gamma\delta A & -B\Gamma A(\delta A-L\delta C) & -B\Gamma A(A-LC) \\ I & 0 & 0 & 0 \\ 0 & I & 0 & 0 \\ 0 & 0 & \delta A-L\delta C & A-LC \end{bmatrix} \begin{bmatrix} x_k \\ x_{k-1} \\ x_{k-2} \\ e_{k-2} \end{bmatrix} \quad (4-17) \quad \blacksquare$$

Remark 4.3: By separating the uncertainty part, the above equation can be expressed in the format of (4-16) with reduced-order state representation (due to the assumption $\delta B=0$) as follows:

$$\tilde{x}_{k+1} = (\tilde{V} + \delta\tilde{V}) \tilde{x}_k \quad (4-18)$$

where $\tilde{x}_k = [x_k^T \quad x_{k-1}^T \quad x_{k-2}^T \quad e_{k-2}^T]^T$, and

$$\tilde{V} = \begin{bmatrix} A+B\Gamma & 0 & 0 & -B\Gamma A(A-LC) \\ I & 0 & 0 & 0 \\ 0 & I & 0 & 0 \\ 0 & 0 & 0 & A-LC \end{bmatrix}, \quad \delta\tilde{V} = \begin{bmatrix} \delta A & -B\Gamma\delta A & -B\Gamma A(\delta A-L\delta C) & 0 \\ 0 & 0 & 0 & 0 \\ 0 & 0 & 0 & 0 \\ 0 & 0 & \delta A-L\delta C & 0 \end{bmatrix} \quad \blacksquare$$

Remark 4.4: With $\delta B=0$ the effects of δA and δC are to increase the order of the closed loop system by two. ■

5. EXPERIMENTAL VERIFICATION AT A NETWORK TESTBED

The delay compensation algorithm was verified at a network testbed which uses the 10 Mbps IEEE 802.4 linear token passing bus and IEEE 802.2 as the link layer protocol in an ISO compatible network architecture (see Appendix B of [12]). Three terminal interface units, each of which are installed as a pair of cards in the backplane of a microcomputer, serve as the communication link in the network testbed. These host microcomputers can communicate with each other via the network medium or directly by using RS-232C communication ports (at a maximum data rate of 9.6 kbps). These microcomputers are PC-AT compatible under the Disk Operating System (DOS). They are designated as host #1, host #2, and host #3.

The host #3 serves as the network manager. By use of the remaining terminal interface units, namely host #1 and host #2, a traffic load generator (TLG) has been designed to emulate the scenario of a large number of *virtual* stations with varying traffic. These virtual stations form a virtual ring in the sense that a virtual token hops around this ring. All odd-numbered virtual stations are emulated on host #1 and all even-numbered virtual stations on host #2. These two microcomputers communicate with each other via the network. While the real token travels back and forth between hosts #1 and #2, a virtual token hops around this virtual ring to emulate an actual logical ring consisting of a large number of terminals. Although this arrangement does not guarantee the transmission rate of the actual network, it suffices to emulate the randomly distributed

delays between the source and destination terminals. The TLG can emulate any number of virtual stations, and the message inter-arrival time and message length at each station can be arbitrarily selected using the random number generator (RNG) functions that are resident in hosts #1 and #2. In this way, the TLG offers flexibility of generating randomly varying network-induced delays with specified upper bounds.

In the test apparatus, the plant and actuator are represented by a constant-field DC servomotor, and a tacho-generator serves as the sensor for measuring the motor speed. The sensor and actuator are connected to one of the virtual stations in host #1 which provides the hardware and software for the DASH-16 A/D and D/A conversion via direct memory access (DMA). This odd-numbered virtual station is designated as #1 in the emulated logical ring. The controller is located in host #2 and can be designated as any even-numbered virtual station, i.e., the controller station can be arbitrarily located in different positions in the logical ring relative to the sensor/actuator station. Since the host #2 functions as an integral part of the TLG, multitasking operations are needed for concurrent execution of the TLG and controller functions. To avoid this multitasking operation (which is not convenient under the *DOS* environment), the host #3 (which is practically idle during normal operations in the capacity of a network manager) is directly connected (via RS-232C) to host #2 such that host #3 serves as a coprocessor for host #2. The control algorithm is resident in host #3 which receives the sensor data (originally generated by the A/D

converter at host #1) from host #2 and transmits back the control command to host #2. This control command is eventually transmitted via the network medium to host #1 for being fed to the D/A converter as shown in Figure 5-1.

Remark 5-1: The transmission delays of the sensor and control data via RS-232C between hosts #2 and #3 can be viewed as part of the total data processing delay at the controller. ■

Remark 5-2: The time skew between the sensor and controller can be set to any desired value (between 0 and T) via the RS-232C link between hosts #1 and #3 during the initialization of this test facility. ■

The servomotor serves as a continuous-time plant which communicates with its computer controller via the network. This represents a control loop within the ICCS. A relative measure of efficacy of the proposed delay-compensation algorithm is obtained by comparing the performance of a Proportional-Integral (PI) controller without any delay compensation against that of the same controller with delay compensation.

The steady-state characteristics of the plant were experimentally determined as:

$$y_{ss} = \begin{cases} K(u_{ss} - \beta) & \text{for } u_{ss} > \beta \\ 0 & \text{for } -\beta \leq u_{ss} \leq \beta \\ K(u_{ss} + \beta) & \text{for } u_{ss} < -\beta \end{cases} \quad (5-1)$$

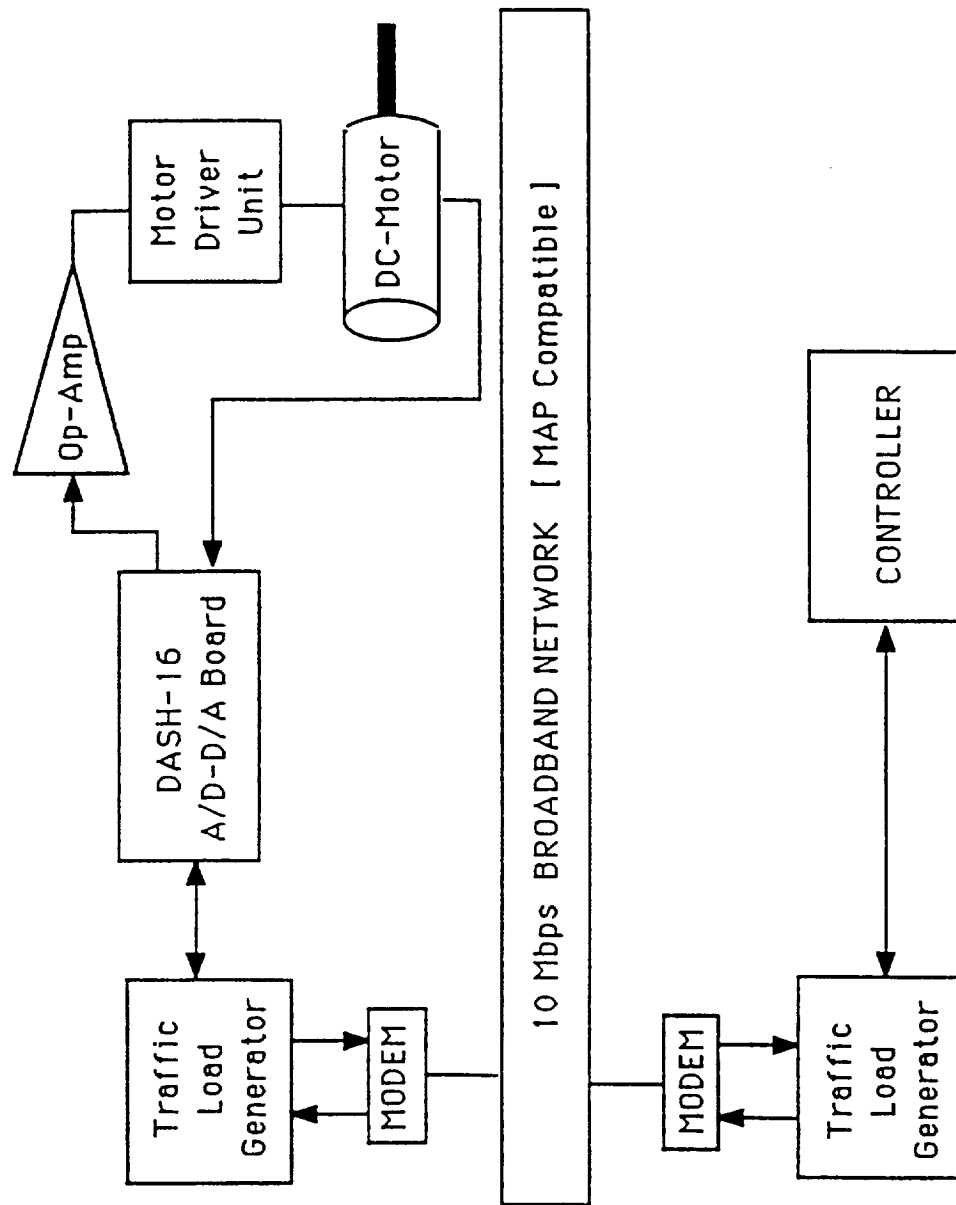


Figure 5-1.. Schematic Diagram of the Experimental Facility.

where y_{ss} = measured steady-state angular velocity of the motor,
 u_{ss} = constant input voltage,
 K = steady-state plant gain, and β = limit of dead band.

In the linear region, the motor dynamics were represented by a first order model after appropriate bias compensation in the control input:

$$x_{k+1} = a x_k + b u_k \quad (5-2)$$

$$y_k = c x_k \quad (5-3)$$

where $a = \exp(-T/\tau)$, T and τ being the sampling period and the motor time constant, respectively,

$$b = \int_{jT}^{(j+1)T} \exp(-((j+1)T-t)/\tau) K dt/\tau = [1-\exp(-T/\tau)]K, \text{ and } c=1.$$

The plant parameters were identified from experimental data to be: $\tau=1.7s$; $K = 3.33$ (rad/s)/volt; and $\beta=3.4$ volts which is equivalent to 11.3 rad/s. The state variable feedback, in this first-order plant, yields a proportional controller where the gain, γ , is obtained by pole placement such that the closed loop pole $p=a-b\gamma$. Similarly the observer gain l is chosen to place the observer pole at $f=a-l$.

Since the plant model is not exact, the observer is expected to generate a steady-state error in the state estimate. Therefore, a weak integral action was used to compensate for this possible

steady-state error. The integral gain was set, by trial and error, between 0.09 and 0.15 volt/(rad/s) to provide zero steady-state error for a variety of induced delays.

Two different experimental setups were considered. The first experimental setup was oriented towards determining the efficacy of the delay compensation algorithm when the total delay in the control loop is a constant with magnitude equal to an integer number of sampling periods. The second experiment emulated an *ICCS* environment by using randomly varying delays. The objective of the second experiment was to examine the robustness of the observer-based compensator due to data rejection and vacant sampling [11,12] coupled with plant modeling uncertainties and nonlinearities.

5.1. Experimental Setup #1: Velocity Control with Constant Delays

The objective of this experiment was to investigate the performance of the uncompensated and compensated control systems of the servomotor with deterministic delays such that a constant bound of p sampling periods could be strictly enforced. This was accomplished by setting: (i) the number of virtual stations to a minimum of two; (ii) network-induced delays to desired values by adjusting the emulated traffic; and (iii) the time skew between (co-located) sensor and actuator sampling instants to zero. This arrangement is equivalent to generating a constant delay by storing the incoming data from the A/D converter into a FIFO, push-pop buffer of size p .

Remark 5-4: From Proposition 3.1 in Section 3, it follows that the observer should behave identically for $p=0$ and $p=1$ for constant gains Γ and L provided that the plant model is exact. ■

Remark 5-5: Since the plant under test is nonlinear, the dynamic characteristics of the control system are a function of the reference input. ■

Figure 5-2 compares the response of the compensated control system with that of the control system without the observer when the delay was zero, and a step change of 16 rad/s in the reference velocity was applied from 0 rad/s. The controller and observer poles were set at $p=0.5s^{-1}$ and $f=0.15s^{-1}$, respectively, the integral gain of the PI controller to 0.15 volt/(rad/s), and the sampling period to 0.3s. The maximum input to the motor was restricted to 10 volts to avoid any potential damage; this corresponds to a steady state velocity of about 22 rad/s.

As expected, the performances of the system with and without the compensator were comparable for zero delay. In this case, the observer-based controller suffered from the error in state estimation. The tracking properties of the observer can be improved by feeding in well-structured information about the plant nonlinearities. For instance, the input to the observer can be modified as follows:

$$u_{ob} = \begin{cases} u_{con} - \beta/K & \text{if } u_{con} > \beta/K \\ 0 & \text{if } |u_{con}| \leq \beta/K \\ u_{con} + \beta/K & \text{if } u_{con} < -\beta/K \end{cases} \quad (5-4)$$

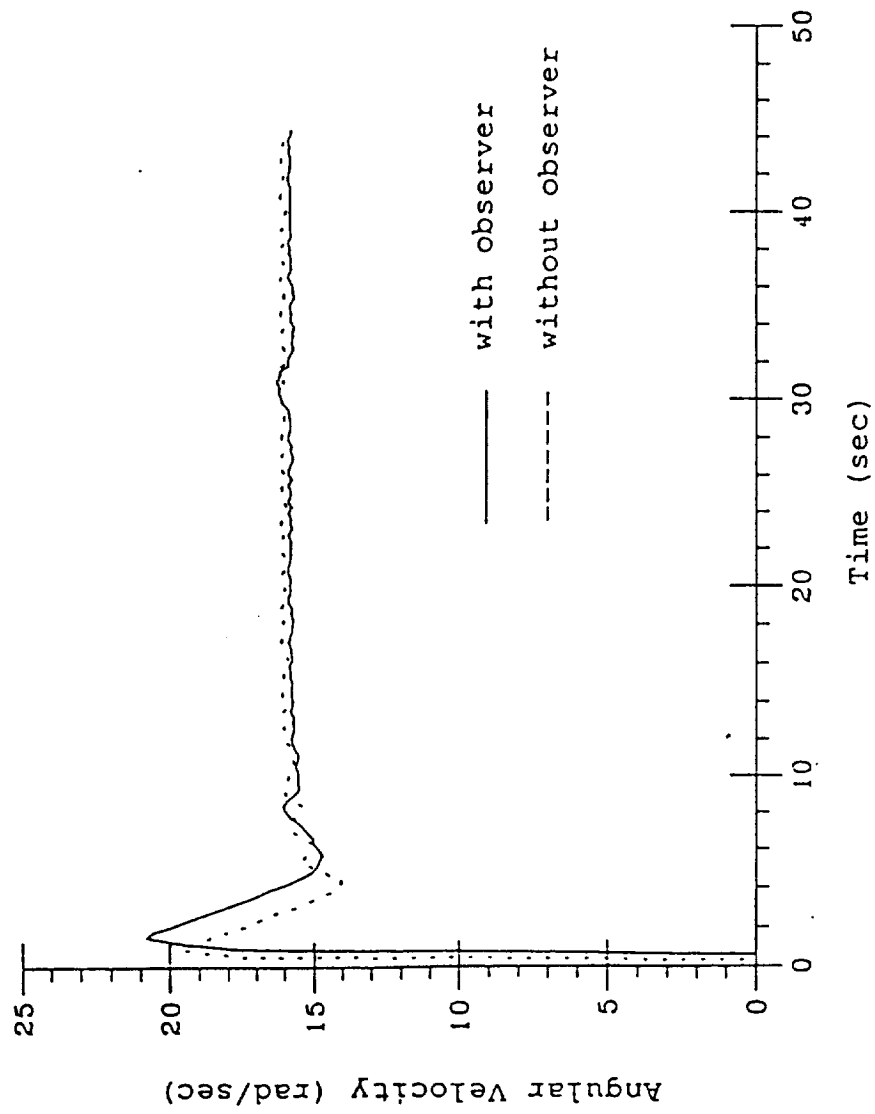


Figure 5-2. Dynamic Response of the Motor:
Fixed Delay = 0, Reference Velocity = 16 rad/sec

where u_{ob} is the modified input to the observer and u_{con} is the actual input to the DC motor. This empirical modification mimics the nonlinearities in the steady-state characteristics of the servomotor by adding *a priori* known information about the bias to the observer in the form of an input, and does not increase the order of the observer. Results, to be presented next, indicate that the steady state tracking errors were practically eliminated in this modified system. With the above modifications, the controller and observer poles were reset at $p=0.1s^{-1}$ and $f=0.0$, respectively, the integral gain to 0.09 volt/(rad/sec), and the sampling period was retained at 0.3s.

Remark 5-6: The above parameter settings were tested, by trial and error, to yield best responses of this nonlinear system for different delays. ■

Remark 5-7: In general, setting the observer pole at zero, i.e. making the observer to be deadbeat, is not a recommended practice because of possible noise amplification. The integral action, enforced in this experiment, should act a low pass filter to attenuate the high frequency noise. The response of the compensated system was found to settle down slightly faster than that of the uncompensated system when the delay was zero in both cases [17]. A possible explanation for this phenomenon is that a lead action is provided by the observer with a pole at zero. ■

Experiments were conducted for different combinations of delays and reference velocities. Series of curves comparing the responses of the compensated and uncompensated system are recorded in [17]. We summarize the general information first and then present the selected results in detail.

The performance of the compensated system was always superior to that of uncompensated system for delays of T and $2T$, i.e., one and two sampling periods. For delays of $3T$ and larger, the compensated system generally exhibited significant oscillations, and the uncompensated system performed worse. For example, with a delay of $3T$ at the reference velocity of 17 rad/s, the compensated system response exhibited a limit cycle which was 3 times smaller in magnitude than that in the uncompensated system. The impact of reference input on the nonlinear system is presented next.

Because of the deadband nonlinearity of the servomotor, a sudden jump in the system response was caused whenever the reference input was set close to ≈ 12 rad/s. As the reference input was increased, the dynamic responses of both compensated and uncompensated systems improved regardless of the magnitude of the delay. This is expected because as the reference speed is increased the motor excitation is drawn away from the on-off nonlinearity region. Moreover, the plant model is possibly better represented at higher velocities where the motor voltage versus speed characteristics are more closely follow a straight line pattern. As a result of a dead band in the motor characteristics, limit cycles frequently appeared in the uncompensated system response.

Now we present selected results in Figures 5-3 and 5-4 to show comparisons of dynamic responses of the delay compensated system for delays of T and $2T$ with step changes of 15 rad/s and 13.5 rad/s, respectively, in the reference velocity from 0 rad/sec. The response

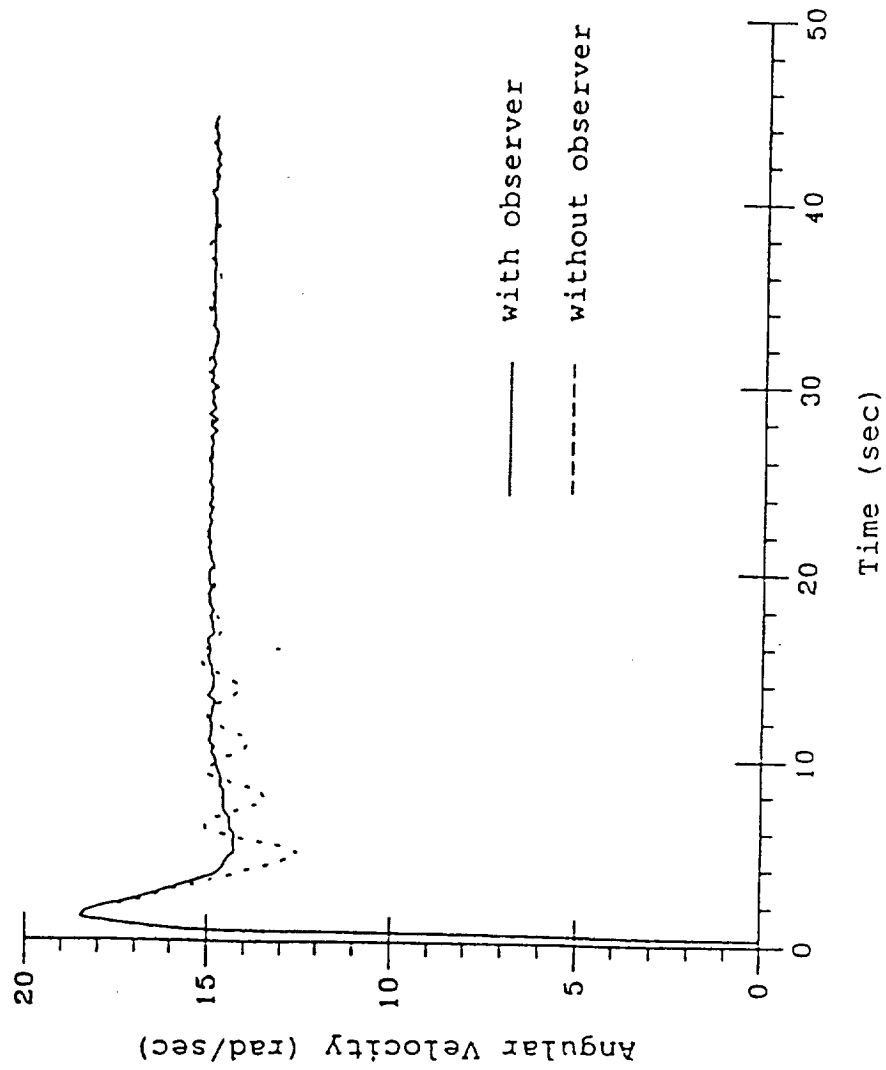


Figure 5-3. Dynamic Response of the Motor:
Fixed Delay = T; Reference Velocity = 15 rad/sec

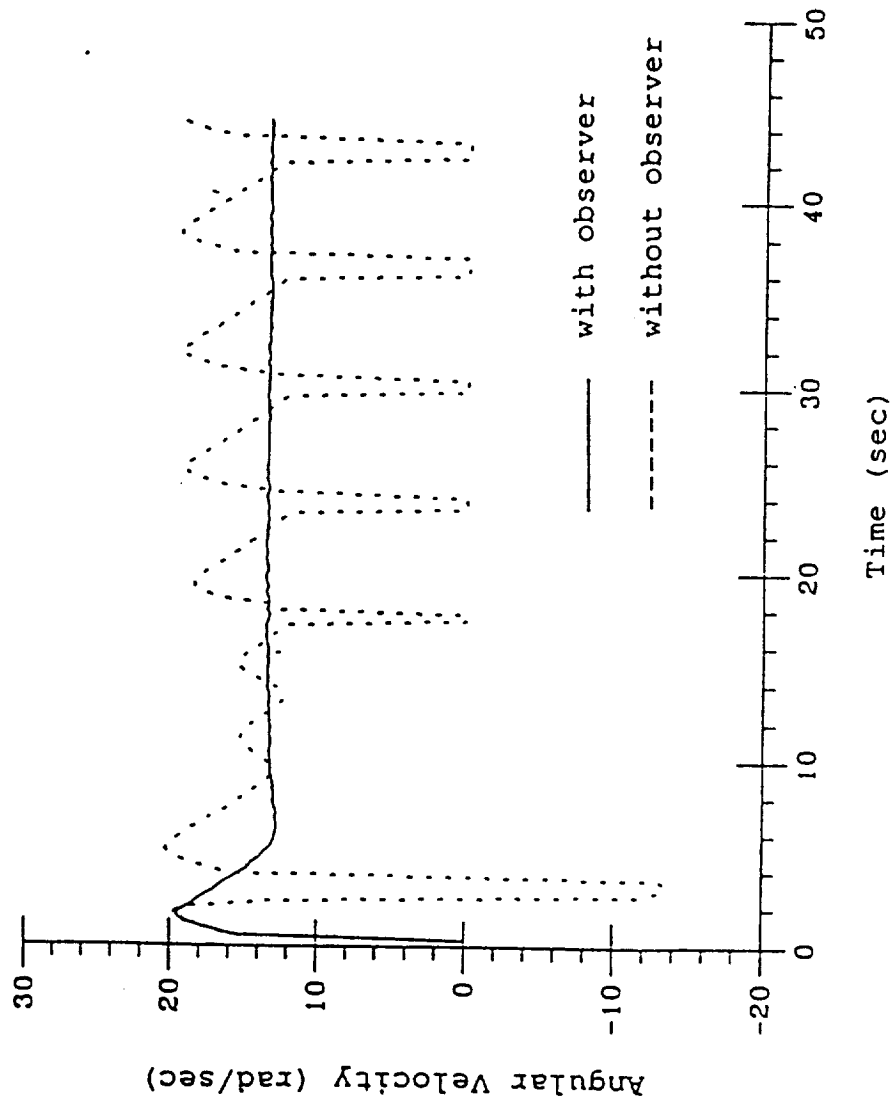


Figure 5-4. Dynamic Response of the Motor:
Fixed Delay = $2T$, Reference Velocity = 13.5 rad/sec

of the compensated system is less oscillatory and evidently superior to that of the uncompensated system in Figure 5-3. The uncompensated system in Figure 5-4 suffered from sustained oscillations because the reference velocity of 13.5 rad/s is close to 12 rad/s when the servomotor tends to stall. In contrast, the compensated system brought the response to the reference point without any noticeable undershoot and thus saved the system from entering into the deadband zone.

Remark 5-8: The predictive properties of the compensator apparently largely eliminate the problems of limit cycling for delays of T and $2T$. Since the above observation relates to a first order plant under specific operating conditions, these experimental results do not provide a definite conclusion regarding robustness of the delay compensator relative to plant modeling uncertainties and nonlinearities in higher order plants. ■

5.2. Experimental Setup #2: Velocity Control with Random Delays

The objective of this experiment was to investigate the performance and robustness of the proposed delay compensation algorithm when the communication network was subjected to random traffic generated from a large number of virtual stations. The control system is likely to be subjected to data rejection and vacant sampling at the controller's receiver buffer [11,12] if the compensator is not used. This problem can be apparently circumvented by an appropriate choice of buffer size, namely p , at the controller and actuator buffer. However, if p is selected to be small, the randomly varying delays would exceed this bound and generate vacant samples with a larger

probability. On the other hand, if p is selected to be large, the impact of randomly varying delays would be reduced at the expense of potential instability due to plant modeling uncertainties and nonlinearities. (Note: If the plant is unstable in the open loop, then it follows from Figure 3-1 that the dynamic error of estimation will be worse with a larger p). Selection of p becomes a design problem which calls for trade-off between mitigating the effects of uncertainties in network traffic and plant modeling.

Setup #2 is similar to setup #1 with the following exceptions:

Number of virtual stations = 30.

Identical traffic distribution at all 28 virtual stations except the sensor and controller. The message arrival process is Poisson with an average inter-arrival time of 0.3s. These virtual stations were assumed to have identical message lengths which were adjusted to keep the offered traffic [6] at 0.5.

In view of additional noise due to randomly varying delays, locations of controller and observer poles were moved back to $p=0.5s^{-1}$ and $f=0.15s^{-1}$, respectively, from the previous values of 0.1 and 0.0. The integral gain was reset to 0.15 volt/(rad/s) from 0.09 to compensate for potentially larger steady-state estimation errors.

In general, the system dynamic response deteriorated under random traffic for both compensated and uncompensated systems [5]. A typical comparison is shown in Figure 5-5 where the response of the compensated system is seen to be superior to that of the uncompensated system. Since the traffic distribution is Poisson, the upper bounds of the network-induced delays can only be set with a certain confidence. Having the bounds of each of the two induced delays set to the sampling period T implies that $p=2$. This causes some of the sensor and controller data to be lost, and yields a steady-state error possibly due to vacant sampling. If it was possible to increase T without appreciably affecting the system dynamics, upper bounds of the induced delays would have larger confidence intervals. Consequently, the probability of exceeding these bounds would be reduced resulting in improved performance of the compensated system.

Remark 5-9: Both compensated and uncompensated systems were less sensitive to data rejection and vacant sampling, when the controller pole was set closer to unity. On the other hand, bringing the controller pole close to unity results in a sluggish system response. Design of the compensated control system under randomly varying delays needs a trade-off between these two opposing requirements. ■

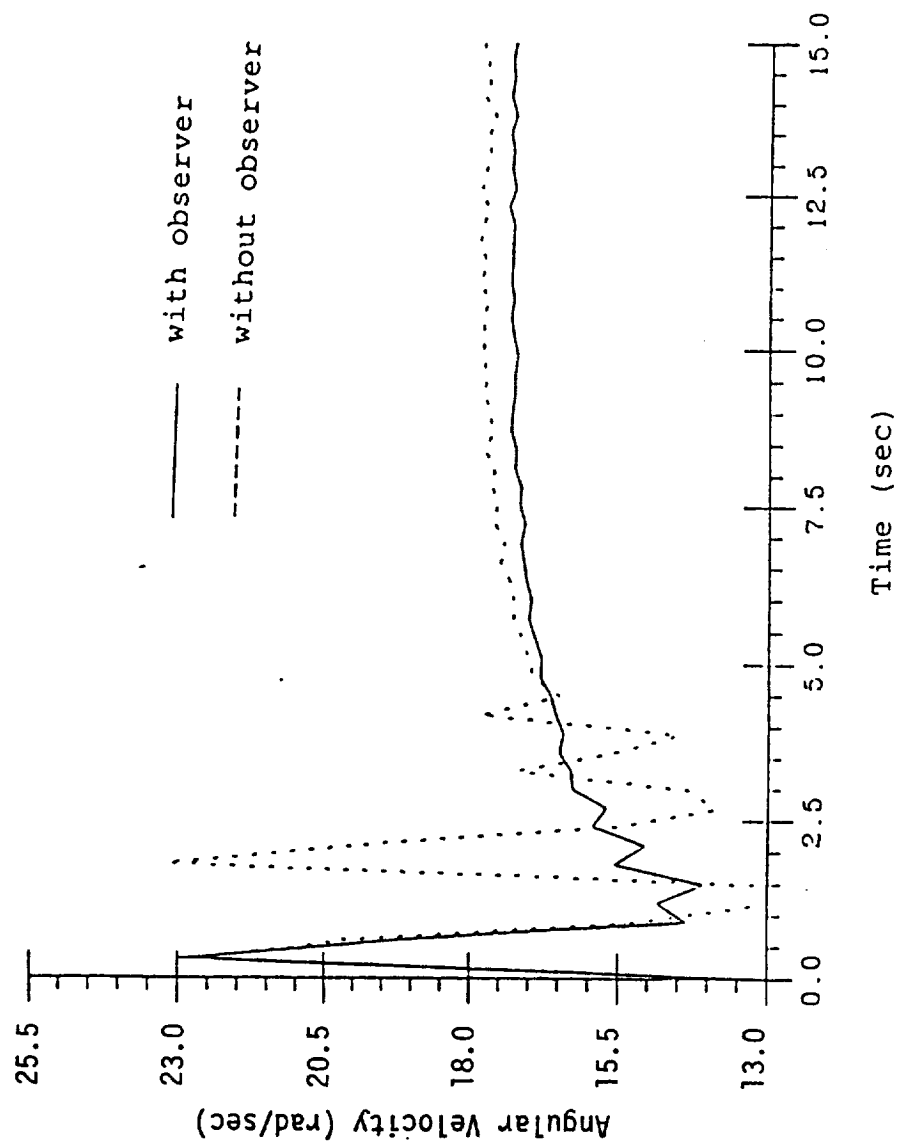


Figure 5-5. Dynamic Response of the Motor:
Random Delay = $2T$, Reference Velocity = 18 rad/sec

6. SIMULATION OF A FLIGHT CONTROL SYSTEM

The delay compensation algorithm was verified by simulation of the longitudinal motion control of an advanced aircraft. The flight control system model and the combined continuous-time and discrete event simulation program were similar to those reported in [2]. Simulation results were generated by augmenting the continuous-time part of the above model with the proposed delay compensation algorithm while the discrete-event model of the network was unchanged.

Simulation results were generated under the following conditions:

The network protocol is the optical version of SAE linear token passing bus with a transmission rate of 100 Mbps.

The network has 30 stations that share the common medium.

Station #1 operates as the sensor terminal, and station #2 as the controller terminal with its transmitter queue handling actuator commands and its receiver queue handling sensor data.

Terminals #1 and #2 have a sampling period of 50ms and constant message lengths with the information part equal to 64 bits.

Time skew (between sensor and actuator sampling instants) to zero.

Random traffic in stations #3 to #30 was identically distributed. The message arrival process is Poisson with an average inter-arrival time of 50ms. These terminals are assumed to have identical message lengths which are adjusted to maintain the offered traffic [27] at any desired level.

A schematic diagram of the flight control system is shown in Figure 6-1. (A discrete version of the controller was implemented in the simulation.) The state-variable model of the plant, excluding the sensor data conversion factor of $180/\pi$, is described below.

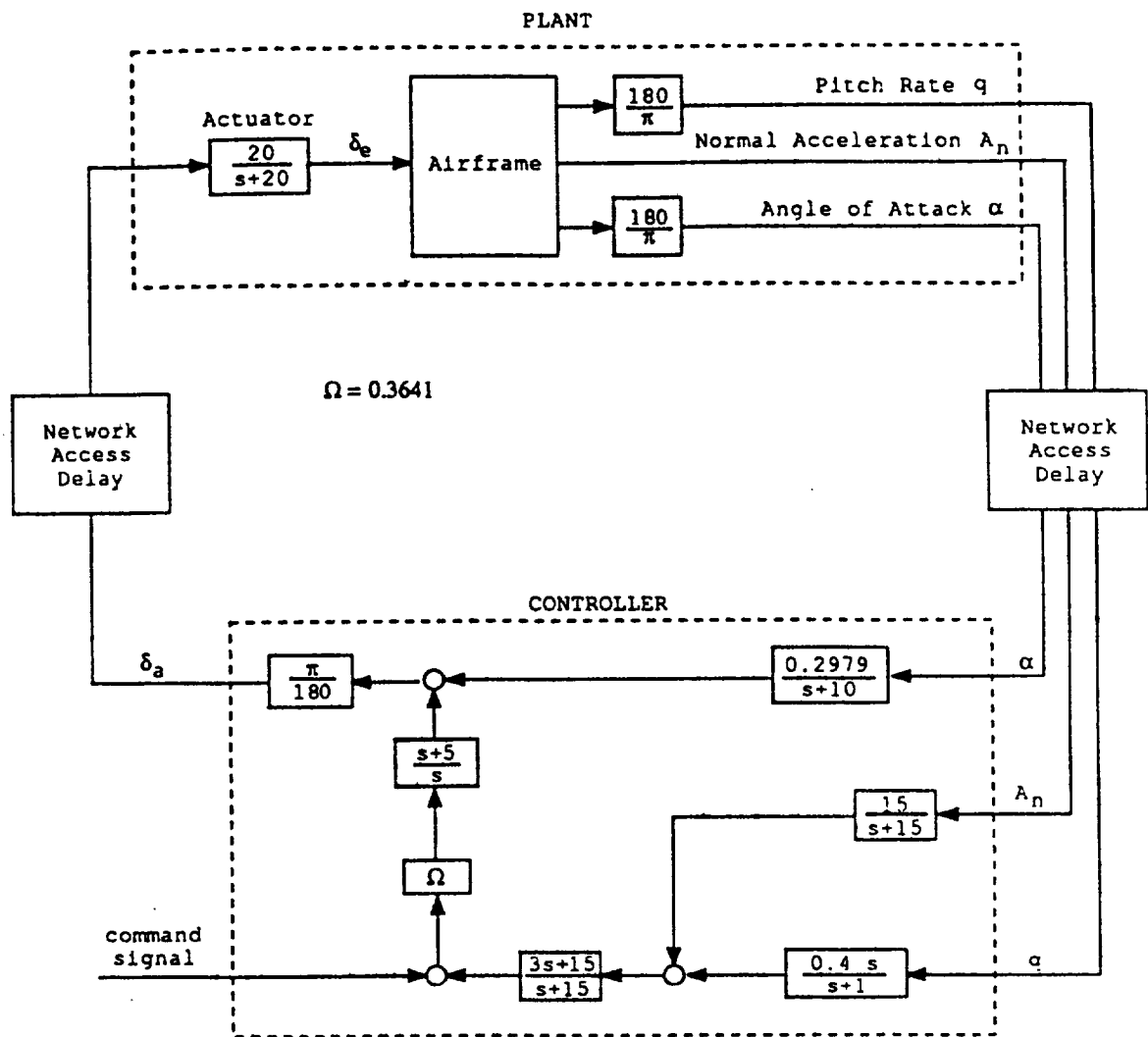


Figure 6-1. Block Diagram of the Flight Control System

Plant Variables and Parameters:

δ_a	= Elevator command, i.e., input to the actuator	(radian)
δ_e	= Elevator deflection, i.e., actuator output	(radian)
W	= Normal component of linear velocity at the center of mass	(ft/s)
Q	= Pitch rate about the center of mass	(radian/s)
α	= Angle of Attack	(radian)
A_n	= Normal component of linear acceleration at the sensor location	(ft/s ²)

The dimensional stability derivatives [2,28] for longitudinal motion dynamics were selected as:

$$\begin{aligned}Z_{de} &:= (\partial Z / \partial \delta_e) / m = -202.28 \text{ ft/s}^2, \\Z_q &:= (\partial Z / \partial Q) / m = -16.837 \text{ ft/s}, \\Z_w &:= (\partial Z / \partial W) / m = -3.1332 \text{ s}^{-1}, \\M_{de} &:= (\partial M / \partial \delta_e) / I_y = -40.465 \text{ s}^{-2}, \\M_q &:= (\partial M / \partial Q) / I_y = -2.6864 \text{ s}^{-1}, \\M_w &:= (\partial M / \partial W) / I_y = -0.01429 (\text{s-ft})^{-1}, \\M_{wd} &:= (\partial M / \partial \dot{W}) / I_y = -0.00115 \text{ ft}^{-1}.\end{aligned}$$

where M is the pitch moment;

Z is the normal component of the aerodynamic force;

m is the lumped mass of the aircraft; and

I_y is the moment of inertia about the pitching axis.

Other constant parameters were:

$$\begin{aligned}
 g &= 32.2 \text{ ft/s}^2 && \text{(Acceleration due to gravity)} \\
 l &= 12.268 \text{ ft} && \text{(Distance between the center of gravity of} \\
 &&& \text{the airframe and the accelerometer)} \\
 r &= 0.05 \text{ s} && \text{(Actuator time constant)} \\
 U_o &= 1005.3 \text{ ft/s} && \text{(Reference flight speed)}
 \end{aligned}$$

Longitudinal Motion Dynamics in the Continuous Time Domain:

$$\frac{dx}{dt} = A x + B u; \quad y = C x \quad (6-1)$$

where $x = [\delta_e \ W \ Q]^T$, $u = \delta_a$, $y = [\alpha \ A_n \ Q]^T$, and

$$A = \begin{bmatrix} -r^{-1} & 0 & 0 \\ z_{de} & z_w & S_0 \\ S_1 & S_2 & S_3 \end{bmatrix}, \quad B = \begin{bmatrix} r^{-1} \\ 0 \\ 0 \end{bmatrix}, \quad C = \begin{bmatrix} 0 & U_o^{-1} & 0 \\ -S_4 & -S_5 & -S_6 \\ 0 & 0 & 1 \end{bmatrix}$$

$S_0 := (z_q + U_o)$, $S_1 := (M_{de} + M_{wd} z_{de})$, $S_2 := (M_w + M_{wd} z_w)$,
 $S_3 := [M_q + M_{wd}(z_q + z_w)]$, $S_4 := (z_{de} + l S_1)/g$, $S_5 := (z_w + l S_2)/g$,
 and

$$S_6 := (z_q + l S_3)/g.$$

The sensor and controller sampling period T was chosen to be 50ms in contrast to 10 ms in [2]. The rationale for selecting a larger value of T was to illustrate how the delay-compensated system would perform relative to the uncompensated system when the sampling rate may have to be reduced to allow for longer processing time for

executing complex control algorithms. This problem might be encountered in future generation hypersonic aircraft.

The observer in the delay compensator was designed in a transformed state space where the three measured outputs α , A_n , and q were made the state variables. All three poles of the discrete-time observer were located at $0.3s^{-1}$. Then the compensator was constructed following the scheme in Figure 3-1 and the control law in Figure 6-1. In the simulation program, the conversion factor of $180/\pi$ as shown in Figure 6-1, was used after the estimated states were computed by the observer.

The dynamic responses of the controller output, angle of attack, normal acceleration, and pitch rate were obtained for a unit step change in the reference signal under different offered traffic in the network. The compensated system response was always less oscillatory than that of the uncompensated system. From the point of view of aircraft control, the benefits of the less oscillatory response are better dynamic response, and reduced control effort and actuator wear.

Figure 6-2 presents dynamic responses of pitch rate for the three cases of non-delayed (i.e., without network-induced delays), delay-compensated, and uncompensated delayed control systems when the offered traffic was set to 0.5. Apparently, the detrimental effects of network-induced delays are partially circumvented and the flight control system response is improved significantly with the use of

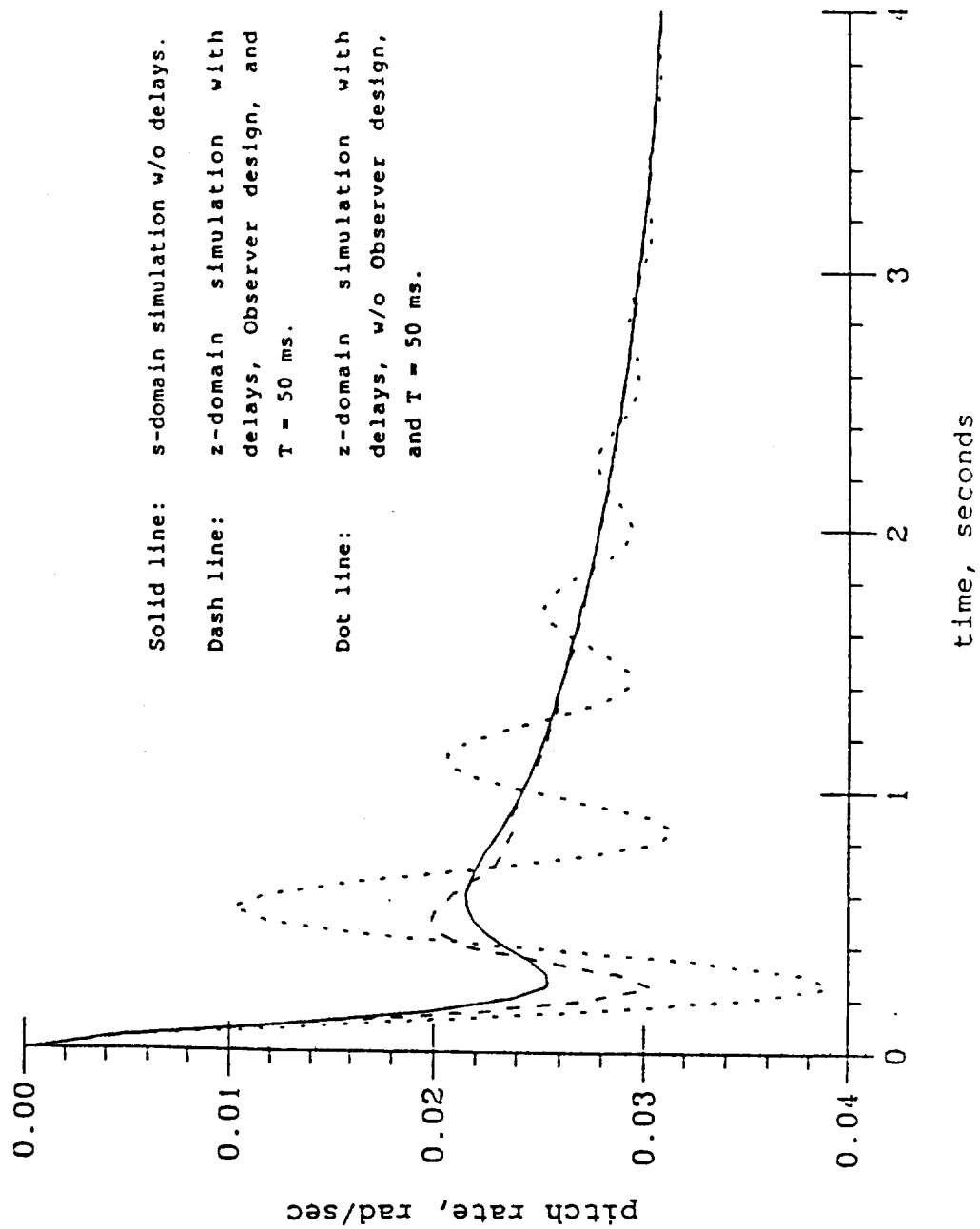


Figure 6-2. Dynamic Response of Pitch Rate

the compensated control scheme. Further research is needed for robustness evaluation of the observer relative to plant modeling uncertainties beyond the analysis presented in Section 4.

Remark 6-1: A common tendency in ICCS design is to increase the sensor sampling rate so as to avoid large delays introduced by the communication network on the tacit assumption that an arbitrarily large bandwidth is available in optical data communication networks. The above assumption may not hold if the network is shared by a large number of control and decision-making functions. Eventually, the increase of network traffic may result in large induced delays for some of the control loops even though the average bus load may remain well below the bandwidth capacity. Following a similar argument, the number of subscribers served by the network would be unduly restricted if the network-induced delays have to be bounded within a very conservative limit. Nevertheless, if appropriate models of the controlled processes are available then, as seen in the experimental and simulation results, the network utilization can be increased by using compensated control systems instead of increasing the sampling rates. The additional computational requirement for the compensator, depicted in Figure 3-1, is expected to be small in comparison to that of the complex algorithms of integrated control systems in the current and future generation advanced aircraft. Therefore, this concept of observer-based delay compensation will allow the controller computers to have less stringent processing power requirements. ■

7. SUMMARY, CONCLUSIONS, AND RECOMMENDATIONS FOR FUTURE RESEARCH

A procedure for compensating the effects of distributed network-induced delays in Integrated Communication and Control Systems (ICCS) has been proposed. The problem of analyzing systems with time-varying and possibly stochastic delays could be circumvented by use of a deterministic observer which is designed to perform under certain restrictive but realistic assumptions.

The proposed delay-compensation algorithm is based on a deterministic state estimator and a linear state-variable feedback control law. The deterministic observer can be replaced by a stochastic observer without any structural modifications of the delay compensation algorithm. However, if a feedforward-feedback control law is chosen instead of the state-variable-feedback control law, then the observer needs to be modified in the same way a conventional non-delayed control system should be. Under these circumstances the delay compensation algorithm would be accordingly changed.

The separation principle of the classical Luenberger observer [26] holds true for the proposed delay compensator.

The proposed delay-compensation algorithm is suitable for Integrated Communication and Control Systems (ICCS) in advanced aircraft, spacecraft, manufacturing automation, and chemical process applications. If the individual components of the ICCS communicate

with each other via a common communication medium, then the network can be designed such that the induced delays are bounded. In this way the detrimental effects of distributed delays induced by the network can be circumvented by the compensator.

As the first step to robustness analysis, the impact of modeling uncertainties, i.e., errors in the plant model matrices, on the performance of the delay-compensated system has been investigated. Further analytical research is recommended following the established techniques for robustness and stability [29-32].

This report has addressed the concept, analysis, implementation, and verification of an algorithm for compensation of network-induced delays that occur in Integrated Communication and Control Systems (ICCS). As reported in Section 3, this algorithm has been developed on the basis of a deterministic state estimator, a multi-step predictor, and a linear state-variable feedback control. The proposed delay-compensation algorithm is suitable for ICCS in large-scale processes like advanced aircraft, spacecraft, autonomous manufacturing plants, and chemical plants. The communication network, that interconnects the individual subsystems and components of the ICCS, should be designed such that the induced delays are bounded relative to a specified confidence interval. In this way the detrimental effects of the distributed and varying network-induced delays can be (at least partially) circumvented by the compensator. The impact of modeling uncertainties, i.e., errors in the plant model matrices, on dynamic performance and stability of the closed

loop compensated system has been investigated for a two-step delayed system. Given the specifications of the control system, the above approach has a potential for establishing bounds on the modeling errors.

Implementation of the delay-compensation algorithm, followed by experimental and simulation results have been presented. Experimentation with a DC-motor in a network testbed assembly has demonstrated that the observer-predictor functions in presence of plant modeling uncertainties, nonlinearities and disturbances, and measurement noise. Simulation of the flight control system of an advanced aircraft within a network environment also shows that the delay compensator is capable of improving the system dynamic performance. However, further analytical and experimental research beyond those reported in this report is needed to enhance robustness of this delay compensator.

Possible areas for future research in the evolving field of Integrated Communication and Control Systems are innumerable. Some of the topics related to the research reported in this report are furnished below.

Research Topic #1: Stochastic Filtering

A stochastic filter can be designed to accommodate the effects of varying delays. The following formulation can be used to specify the filter requirements. Let the plant model be described as

$$x_{k+1} = A_k x_k + B_k u_k + n_k \quad y_k = C_k x_k + v_k$$

where the plant and measurement noises, n_k and v_k , are assumed to be white, mutually independent, and of covariances Q and R , respectively. The delayed sensor data w_k , as input to the filter, is represented as:

$$w_k = \delta_0(\phi_k) y_k + \delta_1(\phi_k) y_{k-1} + \delta_2(\phi_k) y_{k-2} + \dots + \delta_{p-1}(\phi_k) y_{k-p+1}$$

or, alternatively, as

$$w_k = \delta_0(\phi_k) C_k x_k + \delta_1(\phi_k) C_k x_{k-1} + \dots + \delta_{p-1}(\phi_k) C_k x_{k-p+1} + v_k.$$

where $\delta_i(j)$, $i, j=0, 1, 2, \dots, p-1$ is the Kronocker delta defined as

$$\delta_i(j) = \begin{cases} 1 & \text{if } i=j \\ 0 & \text{if } i \neq j \end{cases}, \text{ and}$$

the network-induced parameter ϕ_k is a stochastic chain defined as:

$$\phi_k = \phi(k, \omega) : \mathbb{N} \times \Omega \rightarrow \{0, 1, 2, \dots, p-1\},$$

with \mathbb{N} and Ω representing the above finite set of non-negative integers and the sample space, respectively.

The objective is to obtain the estimate, \hat{x}_k , of the state x_k , which minimizes the performance index

$$J = E\{[\hat{x}_k - x_k]^T M [\hat{x}_k - x_k] \mid W_k\}$$

where W_k is the collection of past measurements $\{w_0, w_1, \dots, w_k\}$,

$E\{\cdot \mid W_k\}$ is the conditional expectation given W_k , and

M is a positive semi-definite weighting matrix.

The above algorithm, formulated with $p=2$, can be applied to the problem of sequential state estimation of discrete processes with interrupted observations. Sawagari et al. [33] proposed a similar formulation but the input to the filter was formulated, with $p=2$, as:

$$w_k = \delta_0(\theta_k) C_k x_k + v_k.$$

In the case of missing data, a filter based on the proposed formulation may yield better results than that obtained by Sawagari et al. Particularly, the approach of Sawagari et al. may not be effective if x_k is under steady state conditions because, assuming that v_k is small, w_k would oscillate between 0 and $C_k x_k$. On the other hand, in the proposed formulation, w_k can vary only between $C_{k-1} x_{k-1}$ and $C_k x_k$.

Research Topic #2: Robust Compensator Design using LQG/LTR

The performance robustness and stability of the control system would be affected by insertion of the delay compensator in the loop. Having designed the optimal state feedback gain Γ , the observer gain L in the compensator needs to be tuned so that the overall system performance is optimal under plant modeling uncertainties, process disturbances, and measurement noise. Linear Quadratic Gaussian (LQG) using Loop Transfer Recovery (LTR) [31,32] is a potential candidate for designing the delay compensator.

Research Topic #3: Optimization of Control and Network Parameters

A cursory treatment on optimization of network-induced delays and associated parameters has been given in Section 4 of [12] for two special configurations of the control system: One is the case of identical sampling frequency of the sensor and controller within a feedback control loop; the other addresses the situation where the sensor sampling frequency is larger than that of the controller, which is a viable option for ICCS design.

For identical sampling, the critical network parameter is Δ , the time skew between the instants of sensor and controller samplings, which is a very slowly varying parameter. Therefore, Δ should be periodically adjusted to maintain optimal performance of the delayed control system. The control law designed with the assumption of a fixed delay may not perform satisfactorily when the system is subjected to network-induced delays. Furthermore, as the characteristics of network traffic change, the induced delays would vary. Consequently, the controller parameters and the time skew Δ should be updated. Therefore, the objective is to derive an optimal control law for a system that is subjected to network-induced delays under varying network traffic. Although research addressing optimal control has been reported for systems with transportation lag [34,35], the simultaneous optimization of control and network parameters, namely the state-variable feedback matrix F and time skew Δ , has not been apparently attempted before. Future research may make use of the model derived in [11].

For the alternative approach of non-identical sampling [12.13], the research problem is identification of an optimal sampling ratio ϵ , which minimizes a specified performance index and guarantees stability of the closed loop control system under given network traffic statistics and a fixed controller sampling period.

Research Topic #4: Selection of the Number of Predictor steps

The delay compensation algorithm, presented in this report, does not take into account the effects of recurrent loss of sensor and/or control data in the network. (See Remark 3.2 and Appendix A). The compensated system is expected to perform in a gracefully degraded mode if the system remains observable and reachable under recurrent loss of data. The number, p , of predicted steps may be required to be increased to accommodate this feature. Selection of p is dictated by uncertainties in both network traffic and plant modeling.

APPENDIX A

EXTENDED OBSERVABILITY UNDER RECURRENT LOSS OF OUTPUT DATA

An observable (reachable) system that assumes availability of sensor (control) data at consecutive samples may become unobservable (unreachable) due to recurrent loss of data in the computer network. If the control system is unstable in the open loop as it could be for highly maneuverable supersonic aircraft, then recurrent loss of data could render the system undetectable and/or unstabilizable.

The concept of state estimation with recurrent loss of sensor data has been addressed by other investigators in different contexts. For example, Sawagari et al. [33] and Jaffer and Gupta [36] considered the problem of sequential estimation with interrupted observations within a stochastic setting. The sequential state estimation algorithms in both cases are developed using a Bayesian approach. To the best of the authors' knowledge, the problem of observability under persistent and random loss of data has not been studied before.

This appendix introduces the concept of extended observability under recurrent loss of data where the state vector has to be reconstructed from an ensemble of sensor data at non-consecutive samples. Given that the computer network is designed to keep the probability of losing more than m data in every set of $(\nu+m)$ successive data less than an *a priori* prescribed bound ρ , the problem is to establish test criteria for observability (reachability) under

this condition. ν is the observability (reachability) index, and m is known as a function of p and ν . A fixed-size window of $(\nu+m)$ data from the available collection is considered for each observation, and sample numbers of the missing data are routinely recorded by the computer network protocol. This concept is different from that of extended observability with unknown inputs, for example, Basile and Marro [37], Emre and Silverman [38], Kudva et al. [39], Molinari [40], and Rappaport and Silverman [41].

The extended observability can be determined by testing the rank of every possible matrix associated with an augmented set of output data arising from each possible combination of data loss. Although this test is exhaustive, it is time-consuming, in general, and could lead to incorrect conclusions due to computational inaccuracy. An alternative approach for determining extended observability in the single-output case is presented. The relevance of the work reported in this appendix is summarized below:

- o A necessary and sufficient condition for extended observability which can be expressed via a recursive relation.
- o Necessary conditions (for the above) that are related to the characteristic polynomial of the state transition matrix in a discrete-time setting, or of the system matrix in a continuous-time setting.
- o A system-theoretic approach for having an insight into the problem of loss of observability.

A.1. Extended Observability: Concepts and Test Criteria

Let the plant be represented by a discrete-time, linear, time-invariant model in a deterministic setting at the sampling instant k

$$x(k+1) = A x(k) + B u(k); \quad z(k) = C x(k) \quad (A-1)$$

where the state vector $x \in R^n$, the input vector $u \in R^r$, the output vector $z \in R^p$, and the constant matrices A , B , and C are of compatible dimensions. Furthermore, rank of C is p and the pair (C,A) is observable with observability index ν . Then,

$$x(k+j) = A^j x(k) + \sum_{i=0}^{j-1} A^i B u(k+j-1-i) \quad (A-2)$$

Defining $y(k+j) = CA^j x(k)$, it follows from (A-1) and (A-2) that

$$y(k+j) = z(k+j) - \sum_{i=0}^{j-1} C A^i B u(k+j-1-i) \quad (A-3)$$

The modified output vector sequence $\{y(k)\}$ can be used for state reconstruction in lieu of $\{z(k)\}$ provided that the input sequence $\{u(k)\}$ is available. (Observability with unknown inputs [37,41] is not addressed here.) Under normal circumstances, the state x can be reconstructed from ν consecutive sets of outputs. However, in the event of loss of outputs, $y(k)$ is not available at every k . The problem is to determine whether the state $x(k)$ can be reconstructed by selecting *any* ν output vectors from the collection $Y^m(k)$ of $(\nu+m)$ output vectors as defined below. (Note: $Y^m(k)$ may also be viewed as a $(p(\nu+m) \times 1)$ vector.)

$$Y^m(k) = [y(k)^T \mid y(k+1)^T \mid y(k+2)^T \mid \dots \mid y(k+\nu+m-1)^T]^T$$

where m is a fixed finite integer.

Definition A.1: The system in (A-1) is said to be m -observable if $x(k)$ can be reconstructed from any ν distinct vectors in $Y^m(k)$. ■

We now elucidate the concept of m -observability by second order, single output systems which are observable but not m -observable.

Example A.1: Let A and c be defined as follows.

Given $A = \begin{bmatrix} 0 & -1 \\ 1 & 0 \end{bmatrix}$ and $c = [1 \ 0]$, the observability matrix

$\Theta = \begin{bmatrix} c \\ cA \end{bmatrix} = \begin{bmatrix} 1 & 0 \\ 0 & -1 \end{bmatrix}$ implies that the pair (c, A) is observable.

On the other hand, $cA^2 = [-1 \ 0] = -c$.

The system is not 1-observable and hence, cannot be m -observable, $m \geq 1$. From a geometric point of view, A is a 90° rotation matrix implying that $cA^{\ell+2} = -cA^\ell$ for $\ell=0,1,2,3,\dots$. ■

Example A.2: Next we consider a 120° rotation matrix so that

$$A = \begin{bmatrix} -1/2 & -\sqrt{3}/2 \\ \sqrt{3}/2 & -1/2 \end{bmatrix} ; \quad c = [1 \ 0].$$

This system is 1-observable but not m -observable, $m \geq 2$. ■

Next we proceed to determine the conditions for m -observability. The following relationship between $Y^m(k)$ and $x(k)$ is derived from (A-1), (A-2) and (A-3).

$$Y^m(k) = Qx(k) \tag{A-4}$$

where $Q = [\Theta^T \mid \Theta_m^T]^T$ which is a $(p(\nu+m) \times n)$ matrix,

$\Theta = [(CA^0)^T \mid (CA^1)^T \mid \dots \mid (CA^{\nu-1})^T]^T$, and

$\Theta_m = [(CA^\nu)^T \mid (CA^{\nu+1})^T \mid \dots \mid (CA^{\nu+m-1})^T]^T$

We now establish a simplified necessary and sufficient condition for m -observability.

Proposition A.1: The system described in (A-1) is m -observable in the single output case (i.e., C is a $1 \times n$ row vector c and $\nu=n$) iff all minors of $\theta_m \theta^{-1}$ are non-zero.

Proof: It suffices to show that an arbitrary set of n rows from $Q\theta^{-1}$ contains linearly independent vectors iff all minors of $\theta_m \theta^{-1}$ are non-zero. Consider the $(n+m) \times n$ matrix

$$Q\theta^{-1} = \begin{bmatrix} I_n \\ V \end{bmatrix}, \quad I_n \text{ is the } (n \times n) \text{ identity matrix and } V = \theta_m \theta^{-1} \quad (A-5)$$

Let us choose any $(n-k)$ rows from I_n and any k rows from V . If $k=0$, or $k=n$ for $m \geq n$, this proposition automatically holds. Therefore, we consider $1 \leq k < n$. Let U represent the $(n-k)$ -dimensional subspace spanned by the $(n-k)$ rows selected from I_n and let W represent the subspace spanned by the k rows selected from V . First suppose that all minors of V are non-zero. Having all k -th order non-zero minors implies that any k rows are linearly independent and each linear combination of these rows must have fewer than k zero elements, i.e., more than $(n-k)$ non-zero elements. Therefore, $\dim W = k$ and $W \cap U = \{0\}$. Consequently, any n rows of $Q\theta^{-1}$ are linearly independent. This establishes sufficiency. Next suppose that V contains a zero minor of order k . Then it is possible to construct a linear combination of these rows with at least k zero elements. Such a vector can be expressed as a linear combination of $(n-k)$ rows of I_n .

Therefore this collection of $k+(n-k)=n$ rows of $Q\theta^{-1}$ does not form a linearly independent set. This establishes necessity. ■

Next we relate certain properties of the matrix A in (A-1) to m -observability for the single-output case.

Observation A.1: The matrix $\theta_m \theta^{-1}$ is completely determined by the coefficients of the characteristic polynomial of A . This can be seen by expressing $\theta_m \theta^{-1}$ as follows.

$$\begin{aligned}
 \theta_m \theta^{-1} &= [(cA^n)^T \quad (cA^{n+1})^T \quad \dots \quad (cA^{n+m-1})^T]^T \theta^{-1} \\
 &= [(cA^n \theta^{-1})^T \quad (cA^{n+1} \theta^{-1})^T \quad \dots \quad (cA^{n+m-1} \theta^{-1})^T]^T \\
 &= [(c\theta^{-1} \theta A^n \theta^{-1})^T \quad (c\theta^{-1} \theta A^{n+1} \theta^{-1})^T \quad \dots \quad (c\theta^{-1} \theta A^{n+m-1} \theta^{-1})^T]^T \\
 &= [(cA^n)^T \quad (cA^{n+1})^T \quad \dots \quad (cA^{n+m-1})^T]^T \quad (A-6)
 \end{aligned}$$

where $A = \theta A \theta^{-1}$ and $c = c \theta^{-1}$. ■

This represents a similarity transformation into the standard observability canonical form [26] as follows.

$$\text{where } A = \begin{bmatrix} 0 & 1 & 0 & \dots & 0 \\ 0 & 0 & 1 & \dots & 0 \\ \vdots & \vdots & \vdots & \ddots & \vdots \\ 0 & 0 & 0 & \dots & 1 \\ -a_0 & -a_1 & -a_2 & \dots & -a_{n-1} \end{bmatrix}, \text{ and } c = [1 \ 0 \ 0 \ \dots \ 0] \quad (A-7)$$

Therefore (A-6) depends only on the coefficients of the characteristic polynomial of A . ■

Observation A.2: Following (A-6) and (A-7) in Observation A.1, the first row of $\Theta_m \Theta^{-1}$ is $[-a_0 \quad -a_1 \quad \dots \quad -a_{n-1}]$. By Proposition A.1, a necessary condition for m-observability, $m \geq 1$, is that all 1×1 minors of $\Theta_m \Theta^{-1}$ be non-zero. This implies that each coefficient of the characteristic polynomial of A must be non-zero for m-observability, $m \geq 1$. ■

Observation A.3: The characteristic polynomial of A in Example A.1 is $A^2 + I$, i.e., $a_1 = 0$. Therefore, the system is not m-observable $\forall m \geq 1$. But, the characteristic polynomial in Example A.2 is $A^2 + A + I$, implying that the necessary condition for m-observability is satisfied. ■

Observation A.4: The degree of m-observability is common to all observable pairs that share the same state transition matrix. That is, if $\exists c''$ such that (c'', A) is m-observable, then (c, A) is m-observable for each observable pair (c, A) . The reason for the above is that the output vector c is only required to establish the invertibility of Θ , i.e., observability. On the other hand, given that Θ^{-1} exists, $\Theta_m \Theta^{-1}$ depends solely on the coefficients of the characteristic polynomial of the A-matrix. ■

The test procedure in Proposition A.1 requires computation of the matrix $V = \Theta_m \Theta^{-1}$. We now show how the coefficients of the $m \times n$ matrix V can be recursively computed. From (A-6) and (A-7) it follows that the coefficients of V can be expressed as

$$V(i, j) = V(i-1, j-1) - V(i-1, n) a_{j-1} \quad \text{for } 1 \leq i \leq m \text{ and } 1 \leq j \leq n$$

by setting the initial conditions $V(\cdot, 0) = 0$ and $V(1, j) = -a_{j-1}$. Then,

$$V(i, n) = V(i-1, n-1) - V(i-1, n)a_{n-1} = -\sum_{k=0}^{n-1} a_k V(i-n+k, n)$$

Defining $V_i = V(i, n)$, the above equation can be expressed as

$$V_i = -\sum_{k=0}^{n-1} a_k V_{i-n+k} \quad \text{for } i \geq n \quad (\text{A-8})$$

The range of V_i in (A-8) can be extended by using the relationship

$V_1 = -a_{n-1}$ and defining $V_0 = 1$ and $V_i = 0$ for $i < 0$ as follows.

$$V_i = -\sum_{k=0}^{n-1} a_k V_{i-n+k} \quad \text{for } i \geq 1 \quad (\text{A-9})$$

Using (A-6) and (A-7) the i -th row of V can be expressed as

$$[V(i, 1) \quad V(i, 2) \quad \dots \quad V(i, n)] = cA^{n-1+i} \quad \text{for } i \geq 1 \quad (\text{A-10})$$

Hence, from (A-10) and (A-11), it follows that cA^{n+i} , for $i \geq 0$, can be expressed as

$$cA^{n+i} = -[a_0 \quad a_1 \quad \dots \quad a_{n-1}] \begin{bmatrix} V_i & V_{i-1} & \dots & V_{i-(n-1)} \\ 0 & V_i & \dots & V_{i-(n-2)} \\ : & : & \dots & : \\ : & : & \dots & : \\ 0 & 0 & \dots & V_i \end{bmatrix} \quad (\text{A-11})$$

$$\text{where } V_i = \begin{cases} 0 & \text{for } i < 0 \\ 1 & \text{for } i = 0 \\ -\sum_{k=0}^{n-1} a_k V_{i-n+k} & \text{for } i > 0 \end{cases}$$

Extended observability is critical for design of networked control systems [11-13] especially if the plant under control is unstable in the open loop. This concept is also applicable to bad data

suppression [42] that may lead to random rejection of signals in feedback control systems.

A natural extension of the reported work is to establish test conditions for extended observability in multiple-output systems. This requires the loss of data to be considered from two different perspectives: *Case 1*: The block of data containing the $(p \times 1)$ output vector $z(k)$ is unavailable; and *Case 2*: Only certain elements of $z(k)$ are unavailable at the instant k while the remaining elements could be used for state reconstruction. In the latter case identity of the unavailable outputs may vary with k .

APPENDIX B

Lemmas for Proposition 3.1

This Appendix presents the four lemmas that are necessary to derive the delay compensation algorithm in Proposition 3.1 in Section 3.

Lemma B.1: $z_{k|r} = z_{k|1} - \sum_{i=0}^{r-2} A^i L_{k-i-1} C e_{k-i-1} \quad \text{for } r \geq 2 \quad (\text{B-1.1})$

Proof: The proof of lemma B.1 requires lemmas B.2, B.3, and B.4. We also introduce a definition that will be required to establish recursive relations in the lemmas.

Definition B.1: $f_k := z_{k|1}, \quad g_k := z_{k|2}$

$$G(k, j) := \begin{cases} \sum_{i=0}^{j-1} A^i g_{k-i+1} & \text{for } k \geq j \geq 1 \\ 0 & \text{otherwise} \end{cases}$$

$$F(k, j) := \begin{cases} \sum_{i=1}^j A^i f_{k-i+1} & \text{for } k \geq j \geq 1 \\ 0 & \text{otherwise} \end{cases} \quad \blacksquare$$

By use of Definition B.1 and lemma B.2, it follows that

$$z_{k|r} = G(k-1, r-1) - F(k-1, r-2) \quad (\text{B-1.2})$$

Using the expression for $G(.,.)$ in Definition B.1 in conjunction with lemma B.3, i.e., the equation (B-3.1)), we have

$$\begin{aligned} G(k-1, r-1) &= \sum_{i=0}^{r-2} A^i g_{k-i} = \sum_{i=0}^{r-2} A^i (f_{k-i} - L_{k-i-1} C e_{k-i-1}) \\ &= \sum_{i=0}^{r-2} A^i f_{k-i} - \sum_{i=0}^{r-2} A^i L_{k-i-1} C e_{k-i-1} \end{aligned} \quad (\text{B-1.3})$$

Using the expression for $F(.,.)$ in Definition B.1 in conjunction with (B-1.3), it yields

$$G(k-1, r-1) = f_k + F(k-1, r-2) - \sum_{i=0}^{r-2} A^i L_{k-i-1} C e_{k-i-1} \quad (B-1.4)$$

The proof follows by substituting (B-1.4) and the expression for f_k (from Definition B.1) in (B-1.2). ■

Lemma B.2: Following Definition B.1,

$$z_{k+1}|_r = G(k, r-1) - F(k, r-2) \quad (B-2.1)$$

Proof: The identities $G(k, 1) = g_{k+1}$ and $F(k, 0) = 0$ are obtained from Definition B.1, respectively. Using (B-1.2) in conjunction with these identities yields

$$z_{k+1}|_2 = G(k, 1) - F(k, 0) \quad (B-2.2)$$

Using (3-3) from Section 3 with $r=3$ and $r=2$ and subtracting

$$z_{k+1}|_3 - z_{k+1}|_2 = A(z_k|_2 - z_k|_1) \quad (B-2.3)$$

Using lemma B.3 and (B-2.2) in (B-2.3)

$$\begin{aligned} z_{k+1}|_3 &= G(k, 1) - F(k, 0) + A(g_k - f_k) \\ &= (G(k, 1) + A g_k) - (F(k, 0) + A f_k) \\ &= G(k, 2) - F(k, 1) \end{aligned} \quad (B-2.4)$$

The method of induction is now used to complete the proof of Proposition 3.1. Using (3-3), as in (B-2.3), results in

$$z_{k+1|r+1} - z_{k+1|r} = A(z_{k|r} - z_{k|r-1}) \quad (\text{B-2.5})$$

Substituting (B-2.1) in (B-2.5)

$$\begin{aligned} z_{k+1|r+1} - z_{k+1|r} &= A[G(k-1, r-1) - F(k-1, r-2) - G(k-1, r-2) \\ &\quad + F(k-1, r-3)] \\ &= A[G(k-1, r-1) - G(k-1, r-2)] - A[F(k-1, r-2) - F(k-1, r-3)] \end{aligned}$$

Setting $j=r-1$ in (B-4.1) of lemma B.4 and similarly $j=r-2$ in (B-4.2), and then substituting these results in the above equation, we obtain

$$\begin{aligned} z_{k+1|r+1} - z_{k+1|r} &= [G(k, r) - G(k, r-1)] - [F(k, r-1) - F(k, r-2)] \\ &= [G(k, r) - F(k, r-1)] - [G(k, r-1) - F(k, r-2)] \end{aligned} \quad (\text{B-2.6})$$

Using (B-2.1) in the right hand side of (B-2.6) yields

$$z_{k+1|r+1} = G(k, r) - F(k, r-1) \quad \blacksquare$$

Lemma B.3:
$$z_{k|2} = z_{k|1} - L_{k-1} c_{k-1} \quad (\text{B-3.1})$$

or equivalently,
$$g_k = f_k - L_{k-1} c_{k-1}$$

Proof: From (3-1), (3-2) and (3-6) in Section 3, it follows that

$$z_{k|1} = Az_{k-1|1} + Bu_{k-1} + L_{k-1}Ce_{k-1} \quad (B-3.2)$$

Also, using (3-3), we have

$$z_{k|2} = Az_{k-1|1} + Bu_{k-1} \quad (B-3.3)$$

The proof follows by substituting (B-3.2) in (B-3.3). ■

Lemma B.4:

$$G(k, j+1) - G(k, j) = A[G(k-1, j) - G(k-1, j-1)] \quad (B-4.1)$$

$$F(k, j+1) - F(k, j) = A[F(k-1, j) - F(k-1, j-1)] \quad (B-4.2)$$

Proof:

$$G(k, j+1) - G(k, j) = \sum_{i=0}^j A^i g_{k-i+1} - \sum_{i=0}^{j-1} A^i g_{k-i+1} = A^j g_{k-j+1} \quad (B-4.3)$$

$$G(k-1, j) - G(k-1, j-1) = \sum_{i=0}^{j-1} A^i g_{k-i} - \sum_{i=0}^{j-2} A^i g_{k-i} = A^{j-1} g_{k-j+1} \quad (B-4.4)$$

(B-4.1) is obtained by substituting (B-4.4) into (B-4.3). The proof of (B-4.2) follows a similar procedure. ■

APPENDIX C

Stability of the Delay-Compensated System

This appendix discusses stability of the delay-compensated system in presence of plant modeling errors, as described by (4-15) and (4-16) in Section 4. The objective is to outline an approach for determining a sufficiency condition for stability of the time-varying systems in (4-16) and (4-18).

In this sequel we select a norm of the nominal matrix V such that this norm is close to the spectral radius of V . Thus, if the uncertainty is zero, i.e., $\delta V=0$, a measure of stability margin is provided by this norm that would be close to that of an eigenvalue test. This provides a necessary and sufficient condition for stability of linear time-invariant systems.

Given a matrix $V \in \mathbb{R}^{n \times n}$ and any $\epsilon > 0$ there exists a norm $\|\cdot\|_*$, which is a function of both V and ϵ such that $\rho(V) \leq \|V\|_* \leq \rho(V) + \epsilon$ where $\rho(V)$ is the spectral radius of V , i.e., the magnitude of the largest eigenvalue [43]. The norm is obtained as follows.

Transform V into its Jordan form J such that $V = PJP^{-1}$ where P is an appropriate transformation matrix. Construct a diagonal matrix D with the i^{th} diagonal element equal to ϵ^{i-1} , $0 \leq i \leq n$, and let $Z = PD$. The desired norm is $\|V\|_* = \|Z^{-1}VZ\|_\infty$, that is, the infinity norm of transformation $D^{-1}JD$. Therefore,

$$\|V\|_* = \max_i \sum_{j=1}^n \epsilon^{j-i} |J_{ij}| \quad (C-1)$$

The above equation circumvents the problem of matrix inversion for large n and small ϵ .

It follows that if $\rho(V) < 1$ we can select a small ϵ and use the following inequality to obtain a test for closed loop stability

$$\|X_{k+1}\|_* = \|(V + \delta V(k))X_k\|_* \leq \|V + \delta V(k)\|_* \|X_k\|_* \quad (C-2)$$

Since $\|V + \delta V(k)\|_* = \|Z^{-1}VZ + Z^{-1}\delta V(k)Z\|_\infty$ and $Z^{-1}VZ$ is a constant matrix, the computation burden is on calculating $Z^{-1}\delta V(k)Z$ only.

The selection of the norm $\|\cdot\|_*$ is an attempt to reduce the amount of conservatism that is inherent in norm tests such as those using the natural norm. Indeed, it is possible for a matrix with spectral radius smaller than one to have an Euclidian norm, or any other standard norm, greater than one. In addition, the set

$$E_* = \{\Omega: \|V + \Omega\|_* < 1\} \quad (C-3)$$

constitutes a region in $R^{n \times n}$ such that if $\delta V(k) \in E_*$ for all k , then the control system described in (4-1)-(4-4) is stable. However, it should be noted that that $0 < \epsilon_1 \leq \epsilon_2$ does not necessarily imply that $E(V, \epsilon_2)$ is contained in $E(V, \epsilon_1)$ or vice versa.

REFERENCES

1. Astrom, K.J., Anton, J.J. and Arzen, K.E., "Expert Control," *Automatica*, Vol. 22, No. 3, pp. 277-286, 1986.
2. Hopkins, A.L. et al., "System Data Communication Structures for Active-Control Transport Aircraft," Volume II, NASA Report No. CR 165774, June 1981.
3. Ray, A., "Performance Analysis of Medium Access Control Protocols for Distributed Digital Avionics," *ASME Journal of Dynamic Systems, Measurement and Control*, December 1987, pp. 370-377.
4. Ray, A. and Phoha S., "Research Directions in Computer Networking for Manufacturing Systems," *ASME Journal of Engineering in Industry*, pp. 109-115, May 1989.
5. Ray, A., "Distributed Data Communication Networks for Real-Time Process Control," *Chemical Engineering Communications*, Vol. 65, pp. 139-154, March 1988.
6. Kiencke, U., "A View of Automotive Control Systems," *IEEE Control Systems Magazine*, Vol. 8, No. 4, pp. 11-19, August 1988.
7. Desai, M.N., Deckert, J.C. and Deyst, J.J. "Dual-Sensor Failure Identification Using Analytic Redundancy," *AIAA Journal of Guidance and Control*, Vol. 2, pp. 213-220, May-June 1979.
8. Chow, E.C. and Willsky, A.S., "Analytical Redundancy and the Design of Robust Failure Detection Systems," *IEEE Trans. Aut. Contr.*, Vol. AC-29, pp. 603-614, July 1984.
9. Ray, A. and Desai, M., "A Redundancy Management Procedure for Fault Detection and Isolation," *ASME Journal of Dynamic Systems, Measurement, and Control*, pp. 248-254, September 1986.
10. Luck, R. and Ray, A., "Failure Detection and Isolation of Ultrasonic Ranging Sensors for Robotic Applications," *IEEE Trans. Sys. Man Cyber.*, Vol. 21, No. 1, January/February 1991.
11. Halevi, Y. and Ray, A., "Integrated Communication and Control Systems: Part I -- Analysis," *ASME Journal of Dynamic Systems, Measurement and Control*, pp. 367-373, December 1988.
12. Ray, A. and Halevi, Y., "Integrated Communication and Control Systems: Part II -- Design Considerations," *ASME Journal of Dynamic Systems, Measurement and Control*, pp. 374-381, December 1988.
13. Liou, L-W and Ray, A., "Integrated Communication and Control Systems: Part III -- Non-Identical Sensor and Controller Sampling," *ASME Journal of Dynamic Systems, Measurement and Control*, September 1990.
14. Kwakernaak, H. and Sivan, R., *Linear Optimal Control Systems*, Wiley, New York, 1972.
15. Luck, R., Ray, A., and Halevi, Y., "Observability under Recurrent Loss of Data," *AIAA Journal of Guidance, Control, and Dynamics*, September/October 1991.
16. Luck, R., "An Observer-Based Compensator for Network-Induced Delays in Integrated Communication and Control Systems," *Ph.D. Dissertation in Mechanical Engineering*, The Pennsylvania State University, University Park, PA, August 1989.
17. SAE Linear Token Passing Multiplexed Data Bus Standard, Version 3.0, May 1987.

18. Isermann, R., *Digital Control Systems*, Springer-Verlag, New York, 1981.
19. Marianni, M. and Nicoletti, B., "Optimal Discrete Systems with pure delays," *IEEE Trans. Automat. Contr.*, AC-18, p. 311, 1973.
20. Dröuin, M. et al., "Feedback Control for Linear Discrete-time Systems with Time Delays," *Automatica*, Vol. 21, No. 3, pp. 323-327, 1985.
21. Pyndick, R.S., "The Discrete-Time Tracking Problem with a Time Delay in the Control," *IEEE Trans. Automat. Contr.*, vol. AC-17, pp. 397-398, June 1972.
22. Zahr, K. and Slivnisky, C., "Delay in Multivariable Computer Controlled Linear Systems," *IEEE Trans. Automat. Contr.*, vol. AC-19, pp. 442-443, August 1974.
23. Bhat, K.P.M. and Kiovo, H.N., "An Observer Theory for Time-Delay Systems," *IEEE Trans. Automat. Contr.*, vol. AC-21, pp. 266-269, April 1976.
24. Fairman, F.W., and Kumar, A., "Delayless Observer for Systems with Delay," *IEEE Trans. Automat. Contr.*, vol. AC-31, no. 3, March 1986, pp. 258-259.
25. Anderson, B.D.O. and Moore, J.B., *Optimal Filtering*, Prentice-Hall, Englewood Cliffs, NJ, 1979.
26. Kailath, T., *Linear Systems*, Prentice-Hall, Englewood Cliffs, NJ, 1980.
27. Halevi, Y. and Ray, A., "Performance Analysis of Integrated Communication and Control System Networks," *ASME Journal of Dynamic Systems, Measurement and Control*, September 1990.
28. Etkin, B., *Dynamics of Flight Stability and Control*, John Wiley, 2nd ed., 1982.
29. Thau, F.E. and Kastenbaum, A., "The Effect of Modeling Errors on Linear State Reconstructors and Regulators," *ASME Journal of Dynamic Systems, Measurement, and Control*, pp. 454-459, December 1974.
30. Vidyasagar, M. and Kimura, H., "Robust Controllers for Uncertain Linear Multivariable Systems," *Automatica*, Vol. 22, No. 1, pp. 8-19, 1986.
31. Doyle, J.C. and Stein, G., "Multivariable Feedback Design: Concepts for a Classical Modern Synthesis," *IEEE Trans. on Automatic Control*, Vol. AC-26, No. 1, February 1981, pp. 1-16.
32. Stein, G. and Athans, M., "The LQG/LTR Multivariable Control System Design Method," *Massachusetts Institute of Technology Report No. MIT LIDS-P-1384*, May 1984.
33. Sawagari, Y., Katayama, T. and Fujishige, S., "Sequential State Estimation with Interrupted Observation," *Information and Control*, Vol. 21, pp. 56-71, 1972.
34. Arthur, W.B. and Dreyfus, S.E., "Control of Linear Processes with Distributed Lags Using Dynamic Programming from First Principles," *Journal of Optimization Theory and Applications*, Vol. 23, No. 3, pp. 429-443, November 1977.
35. Dourin, M., Abou-Kandil, H. and Bertrand, P., "Feedback Control of Linear Discrete-time Systems with Time Delays," *Automatica*, Vol. 21, No. 3, pp. 323-327, 1985.
36. Jaffer, A.G. and Gupta, S.C., "Optimal Sequential Estimation of Discrete Processes with Markov Interrupted Observations," *IEEE Trans. Automat. Contr.*, Vol. AC-16, 471-475, 1971.

37. Basile, G. and Marro, G., "On the observability of linear time-invariant systems with unknown inputs," *J. Optimiz. Theory Appl.*, vol. 3. no. 6, 1969.
38. Emre, E. and Silverman, L.M., "K-Observers for Linear Systems with Unknown Inputs," *IEEE Trans. Automat. Contr.*, vol. AC-25, 1980, 779-782.
39. Kudva, P., Viswanadham, N., and Ramakrishna, A., "Observers for Linear Systems with Unknown Inputs," *IEEE Trans. Automat. Contr.*, Vol. AC-25, No. 1, 1980, pp. 113-115.
40. Molinari, B.P., "Extended Control-lability and Observability for Linear Systems," *IEEE Trans. Automat. Contr.*, vol. AC-21, 1976, pp. 136-137.
41. Rappaport, D. and Silverman, L.M., "Structure and stability of discrete-time optimal systems," *IEEE Trans. Automat. Contr.*, vol. AC-16, 1971, pp. 227-233.
42. Kohlas, J., "On Bad Data Suppression," *IEEE Trans. Automat. Contr.*, Vol. AC-17, 1972, pp. 827-828.
43. Fuchs, J.J., "On Good Use of the Spectral Radius of a Matrix," *IEEE Trans. Automat. Contr.*, vol. AC-27, no. 5, pp. 1134-1135, October 1982.

Report Documentation Page

1. Report No. NASA CR-187136		2. Government Accession No.		3. Recipient's Catalog No.	
4. Title and Subtitle Compensation of Distributed Delays in Integrated Communication and Control Systems				5. Report Date August 1991	
				6. Performing Organization Code	
7. Author(s) Asok Ray and Rogelio Luck				8. Performing Organization Report No. None	
				10. Work Unit No. 505-66-71	
9. Performing Organization Name and Address The Pennsylvania State University Mechanical Engineering Department University Park, Pennsylvania 16802				11. Contract or Grant No. NAG3-823	
				13. Type of Report and Period Covered Contractor Report Final	
12. Sponsoring Agency Name and Address National Aeronautics and Space Administration Lewis Research Center Cleveland, Ohio 44135-3191				14. Sponsoring Agency Code	
15. Supplementary Notes Project Manager, John C. DeLaat, Instrumentation and Control Technology Division, NASA Lewis Research Center, (216) 433-3744.					
16. Abstract Advances in aircraft and spacecraft technology demand high-speed and reliable communications between the individual components and subsystems for decision-making and control. This can be accomplished by Integrated Communication and Control Systems (ICCS) which use asynchronous time-division-multiplexed networks. Unfortunately, these networks can introduce randomly varying distributed delays. This paper presents the concept, analysis, implementation, and verification of a method for compensating delays that are distributed between the sensor(s), controller, and actuator(s) within a control loop. With the objective of mitigating the detrimental effects of these network-induced delays, a predictor-controller algorithm has been formulated and analyzed. Robustness of the delay compensation algorithm is investigated relative to parametric uncertainties in plant modeling. The delay compensator has been experimentally verified on an IEEE 802.4 network testbed for velocity control of a DC servomotor. Dynamic performance of the delay compensator has also been examined by combined discrete-event and continuous-time simulation of the flight control system of an advanced aircraft, that uses the Society of Automotive Engineers (SAE) linear token passing bus for data communications. The paper is concluded with several areas of future research in the evolving field of ICCS.					
17. Key Words (Suggested by Author(s)) Engine airframe integration; Control; Avionics; Computer networks; Real time operation				18. Distribution Statement Unclassified - Unlimited Subject Category 08	
19. Security Classif. (of the report) Unclassified		20. Security Classif. (of this page) Unclassified		21. No. of pages 72	
				22. Price* A04	